



## Research article

Biogenic *Salvia* species synthesized silver nanoparticles with catalytic, sensing, antimicrobial, and antioxidant propertiesSana Ihsan<sup>a</sup>, Hajera Gul<sup>a</sup>, Nargis Jamila<sup>a,\*</sup>, Naeem Khan<sup>b,\*\*</sup>, Riaz Ullah<sup>c</sup>, Ahmed Bari<sup>d</sup>, Tan Wen Nee<sup>e</sup>, Joon Ho Hwang<sup>f</sup>, Rehana Masood<sup>g</sup><sup>a</sup> Department of Chemistry, Shaheed Benazir Bhutto Women University, Peshawar, 25000, Khyber Pakhtunkhwa, Pakistan<sup>b</sup> Department of Chemistry, Kohat University of Science and Technology, Kohat, 26000, Khyber Pakhtunkhwa, Pakistan<sup>c</sup> Department of Pharmacognosy, College of Pharmacy, King Saud University, Riyadh, Saudi Arabia<sup>d</sup> Department of Pharmaceutical Chemistry, College of Pharmacy, King Saud University, Riyadh, Saudi Arabia<sup>e</sup> Chemistry Section, School of Distance Education, Universiti Sains Malaysia, 11800, Minden, Penang, Malaysia<sup>f</sup> Nanobio Research Center, Jeonnam Bioindustry Foundation (JBF), Jangseung-gun, Jeollanam-do, 57248, South Korea<sup>g</sup> Department of Biochemistry, Shaheed Benazir Bhutto Women University, Peshawar, 25000, Khyber Pakhtunkhwa, Pakistan

## ARTICLE INFO

## Keywords:

Silver nanoparticles

*S. plebeia**S. moorcroftiana*

Antibiotics

Snacks

Heavy metals

## ABSTRACT

*Salvia* (Lamiaceae family) is used as a brain tonic to improve cognitive function. The species including *S. plebeia* and *S. moorcroftiana* are locally used to cure hepatitis, cough, tumours, hemorrhoids, diarrhoea, common cold, flu, and asthma. To the best of authors' knowledge, no previous study has been conducted on synthesis of *S. plebeia* and *S. moorcroftiana* silver nanoparticles (SPAgNPs and SMAgNPs). The study was aimed to synthesize AgNPs from the subject species aqueous and ethanol extracts, and assess catalytic potential in degradation of standard and extracted (from yums, candies, and snacks) dyes, nitrophenols, and antibiotics. The study also aimed at AgNPs as probe in sensing metalloids and heavy metal ions including  $Pb^{2+}$ ,  $Cu^{2+}$ ,  $Fe^{3+}$ ,  $Ni^{2+}$ , and  $Zn^{2+}$ . From the results, it was found that *Salvia* aqueous extract afforded stable AgNPs in 1:9 and 1:15 (quantity of aqueous extract and silver nitrate solution concentration) whereas ethanol extract yielded AgNPs in 1:10 (quantity of ethanol extract and silver nitrate solution concentration) reacted in sunlight. The size of SPAgNPs and SMAgNPs determined by scanning electron microscopy (SEM) and transmission electron microscopy (TEM) were 21.7 nm and 19.9 nm, with spherical, cylindrical, and deep hollow morphology. The synthesized AgNPs demonstrated significant potential as catalyst in dyes; Congo red (85 %), methylene blue (75 %), Rhodamine B (<50 %), nitrophenols; *ortho*-nitrophenol (95–98 %) and *para*-nitrophenol (95–98 %), dyes extracted from food samples including yums, candies, and snacks. The antibiotics (amoxicillin, doxycycline, levofloxacin) degraded up to 80 %–95 % degradation. Furthermore, the synthesized AgNPs as probe in sensing of  $Pb^{2+}$ ,  $Cu^{2+}$ , and  $Fe^{3+}$  in Kabul river water, due to agglomeration, caused a significant decrease and bathochromic shift of SPR band (430 nm) when analyzed after 30 min. The  $Pb^{2+}$  ions were comparatively more agglomerated and chelated. Thus, the practical applicability of AgNPs in  $Pb^{2+}$  sensing was significant. Based on the results of this research study, the synthesized AgNPs could provide promising efficiency in wastewater treatment containing organic dyes, antibiotics, and heavy metals.

\* Corresponding author.

\*\* Corresponding author.

E-mail addresses: [nargisjamila@sbbwu.edu.pk](mailto:nargisjamila@sbbwu.edu.pk) (N. Jamila), [naeem@kust.edu.pk](mailto:naeem@kust.edu.pk) (N. Khan).<https://doi.org/10.1016/j.heliyon.2024.e25814>

Received 14 July 2023; Received in revised form 25 January 2024; Accepted 2 February 2024

Available online 6 February 2024

2405-8440/© 2024 The Authors. Published by Elsevier Ltd. This is an open access article under the CC BY-NC-ND license (<http://creativecommons.org/licenses/by-nc-nd/4.0/>).

## 1. Introduction

A variety of nanomaterials/nanoparticles (NMs/NPs) due to their unique size, composition, and surface area, are the materials of today's focus. These can be employed in delivery systems, packaging materials, safe food, novel pathogen detection, and disease treatment. In recent decades, due to lower toxicity, specificity, high loading capacity, efficacy, stability, and biocompatibility, NPs have gained popularity as a strategy for treating cancer and drug delivery [1–3]. A variety of NMs/NPs have a wide range of applications in industries, material science, engineering, biomedical imaging, agriculture, biosensing, environmental remediation, pollutants removal, biomarking, and drug administration [4–7].

Organic synthetic dyes are commonly used in textile, plastic, food, and pharmaceutical industries. The industries released a high content of the toxic dyes in wastewater, creating substantial pollution issues such as eutrophication, deoxygenation, and hindrance to the infiltration of sunlight. Hence, the dyes accumulate in ecosystems causing various toxic effects to the exposed organisms. Usually, the accumulated dyes are not easily biodegraded by wastewater treatment of ultrafiltration, chemical, and electrochemical methods. NPs on the other hand, have been efficient in dyes removal from wastewater. In recent years, numerous NPs have attracted growing attentions in organic dyes degradation. The biosynthesized NPs are used as nanocatalysts for the effective removal of dye contaminants [8–10].

Metal NPs (MNPs) can be synthesized using a variety of techniques including chemical vapour deposition, sol-gel method, solution-based synthesis, chemical reduction, photochemical reduction, co-precipitation, reverse micelle formation, electrochemical, high-energy radiation, and laser ablation [11–13]. However, these methods are thought to be expensive, time-consuming, toxic, and eco-unfriendly [14,15]. Therefore, there has always been a need for fast, efficient, and eco-friendly methods for NPs synthesis to reduce the use of harmful and toxic chemicals. Phytosynthesized MNPs using plants, algae, and microbes have attracted remarkable attention in a number of life fields. Green-synthesized MNPs are non-toxic, efficient, and cost- and time-effective [16]. Because to their unique physico-chemical characteristics, they are excellent candidates for chemical and biological sensing. Recently, researchers found that green MNPs made from medicinal plants have effective antioxidant, antimicrobial, and anti-cancer potential.

Among MNPs, silver nanoparticles (AgNPs) are used in a variety of industries including food, healthcare, and engineering [17]. Many plant parts such as fruits, stems, peels, leaves, and flowers can be used to synthesize AgNPs. They are chemically stable with significant catalytic potential in dyes and antibiotics degradation, detection of toxic contaminants in a wide range of environmental samples, and bactericidal and fungicidal activities [18,19]. Due to unique characteristics and wide potential, AgNPs are used in a number of consumer items, for example, plastics, soaps, foods, fabrics, and pastes [20].

*Salvia*, a largest genus of Lamiaceae family, can be widely found in Pakistan. *Salvia plebeia* (*S. plebeia*), rich in polyphenols and terpenoids is locally used to treat hepatitis, cough, tumours, and diarrhoea with potential antioxidant, antibacterial, antiviral, anti-inflammatory, and anti-cancer activities. Another specie; *Salvia moorcroftiana* (*S. moorcroftiana*) largely distributed in Pakistan is traditionally used to heal hemorrhoids, coughs, and other ailment. It is a rich source of flavonoids and diterpenoids with significant anticancer activities [21–23].

Hence, considering the medicinal importance of the subject species and a wide application of green synthesized AgNPs, the current study was proposed to synthesize AgNPs using *S. plebeia* and *S. moorcroftiana* (SPAgNPs and SMAgNPs) extracts under the experimental conditions of quantity of reducing/stabilizing/capping agent (extract), silver ion concentration (silver nitrate salt), reaction time, stirring, heating, sunlight, and heating. The study also investigated the effect of pH, temperature, and salts on AgNPs stability. The synthesized AgNPs were applied as nanocatalyst to degrade standard dyes; Congo red (CR) methylene blue (MB), Rhodamine B (RdB), (methyl orange (MO), nitrophenols; *ortho*-nitrophenol (ONP) and *para*-nitrophenols (PNP), dyes extracted from food samples (yums, candies, and snacks), and antibiotics; amoxicillin (AMX), doxycycline (DXC), levofloxacin (LFX). Furthermore, the synthesized AgNPs were applied as probe in sensing of metals/heavy metals such as lead ( $Pb^{2+}$ ), copper ( $Cu^{2+}$ ), nickel ( $Ni^{2+}$ ), iron ( $Fe^{3+}$ ), and zinc ( $Zn^{2+}$ ) in river water samples. Additionally, antioxidant and antimicrobial potential of the synthesized AgNPs were assessed.

## 2. Materials and methods

### 2.1. Samples collection

*S. plebeia* was collected from Tirah, Khyber Pakhtunkhwa (Pakistan) in September 2019. *S. moorcroftiana* was collected from a village Zarki Nasratti (site Murri Saam) of District Karak, Khyber Pakhtunkhwa (Pakistan). The samples were cleaned from unwanted solid debris. After that, samples were shade dried at least for a month, powdered, and stored for experimentation in clean and dry plastic bags (Fig. S1, supplementary material). Food samples (branded and unbranded) including different colors of yums, candy sweet balls, and snacks for dyes extraction were collected in triplicate from main local market (Saddar bazaar), Peshawar, Khyber Pakhtunkhwa (Pakistan). To assess the practical applicability of AgNPs as probe for heavy metals detection, real water samples were collected from Kabul river Nowshera, Khyber Pakhtunkhwa (Pakistan). The river water was filtered with 0.22  $\mu m$  syringe filter and stored at 4 °C for further experimentation.

### 2.2. Chemicals, reagents, and instrumentation

For AgNPs synthesis, chemicals including  $AgNO_3$  and extracting solvents (ethanol and ultrapure deionized water) were used. Dyes on which the catalytic activity of the AgNPs was investigated were Congo red, methylene blue, Rhodamine B, methyl orange, and

*ortho*- and *para*-nitrophenols. In addition, to extract dyes from food samples (yums, candies, and snacks), solvent including 70 % ethanol with 2 % ammonia ( $\text{NH}_3$ ) solution and glacial acetic acid (Merck) were procured from authentic suppliers in Peshawar. To determine the catalytic effect of AgNPs in antibiotics degradation, amoxicillin, levofloxacin, and doxycycline were used. To assess the effect of salts on AgNPs stability, and AgNPs as probe in metals sensing, the salts (Merck, Sigma Aldrich) selected were calcium chloride, copper chloride, iron chloride, lead acetate, magnesium chloride, nickel chloride, potassium chloride, sodium chloride, and zinc acetate. Chemicals for assessing antioxidant and antimicrobial activities included 2,2-diphenyl-1-picrylhydrazyl (DPPH), Muller Hinton agar and broth (MHA and MHB), quercetin, gallic acid, bacterial and fungal strains (*Staphylococcus aureus* and *Escherichia coli*, *Candida albicans*, and *Aspergillus flavus*), and reference standards (streptomycin, vancomycin, amphotericin, and fluconazole). Bacterial (*Staphylococcus aureus* ATCC 25923, and *Escherichia coli* ATCC 25922) and fungal (*Aspergillus flavus*, plant pathogen, and *Candida albicans*, ATCC 10231) strains were procured from Applied and Environmental Microbiology Research Laboratory, Quaid-i-Azam University Islamabad.

Production of AgNPs and assessment of antioxidant potential was studied by recording absorbance of the reaction mixtures on UV-Visible spectrophotometer (model UV-1800, Shimadzu, Japan). Functional groups involvement as reducing entities in AgNPs synthesis were identified using FT-IR spectrometer (Bruker model). Size and morphology of AgNPs were analyzed by field emission scanning electron microscope (FE-SEM) (S-4800, Hitachi, Japan). The instrument is equipped with an ExB in-lens filter, Thermo-NORAN NSS EDS, cold field emission electron gun, resolution 1 nm at 15 KV, 1.4 nm at 1 KV, magnification 20X to 800,000X, imaging

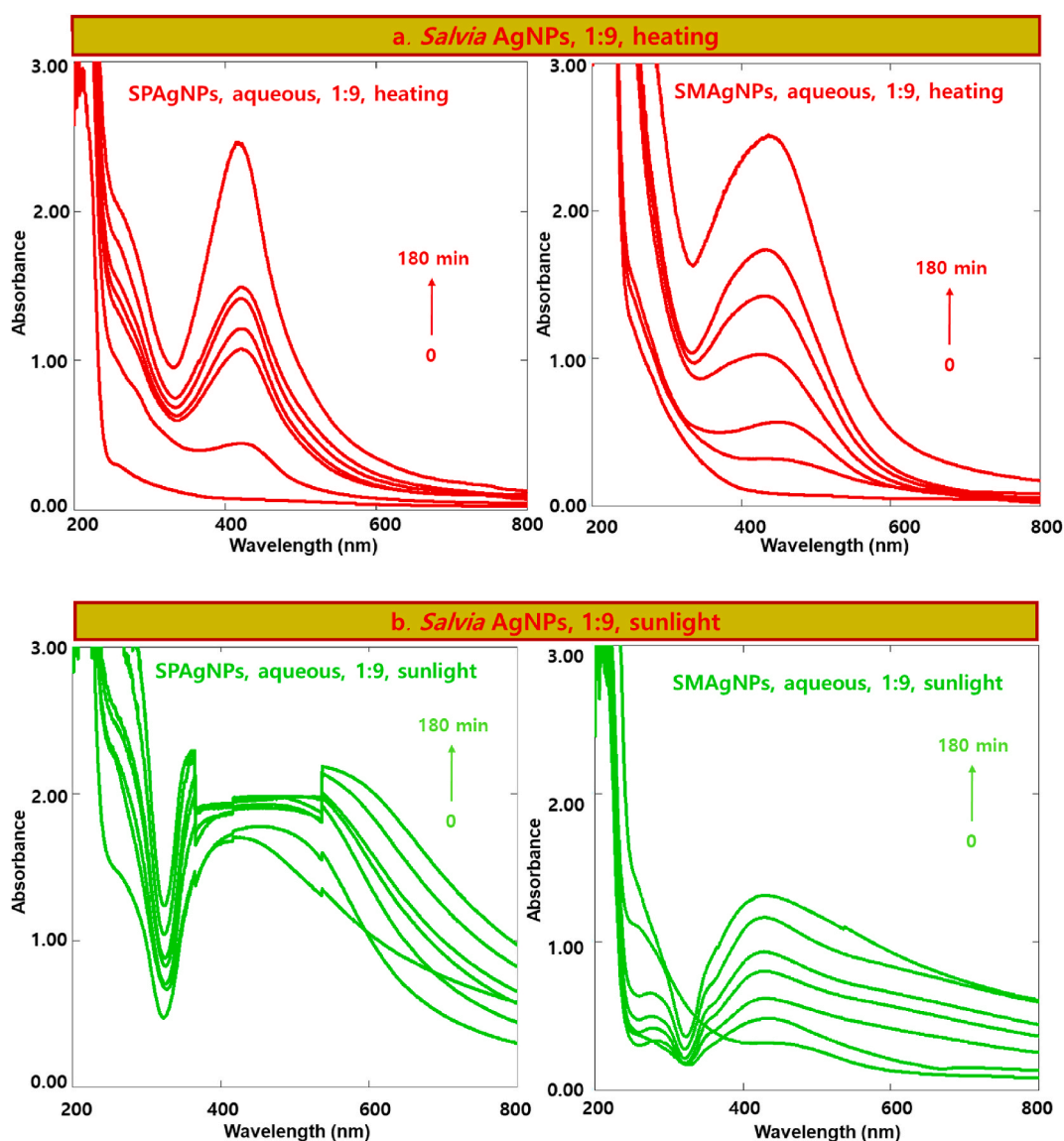


**Fig. 1.** Successive UV-Vis absorption spectra (200–800 nm) of aqueous extract mediated SPAgNPs and SMAgNPs synthesis in 1:9 under (a) heating (b) sunlight, (c) stirring, and (d) incubation.

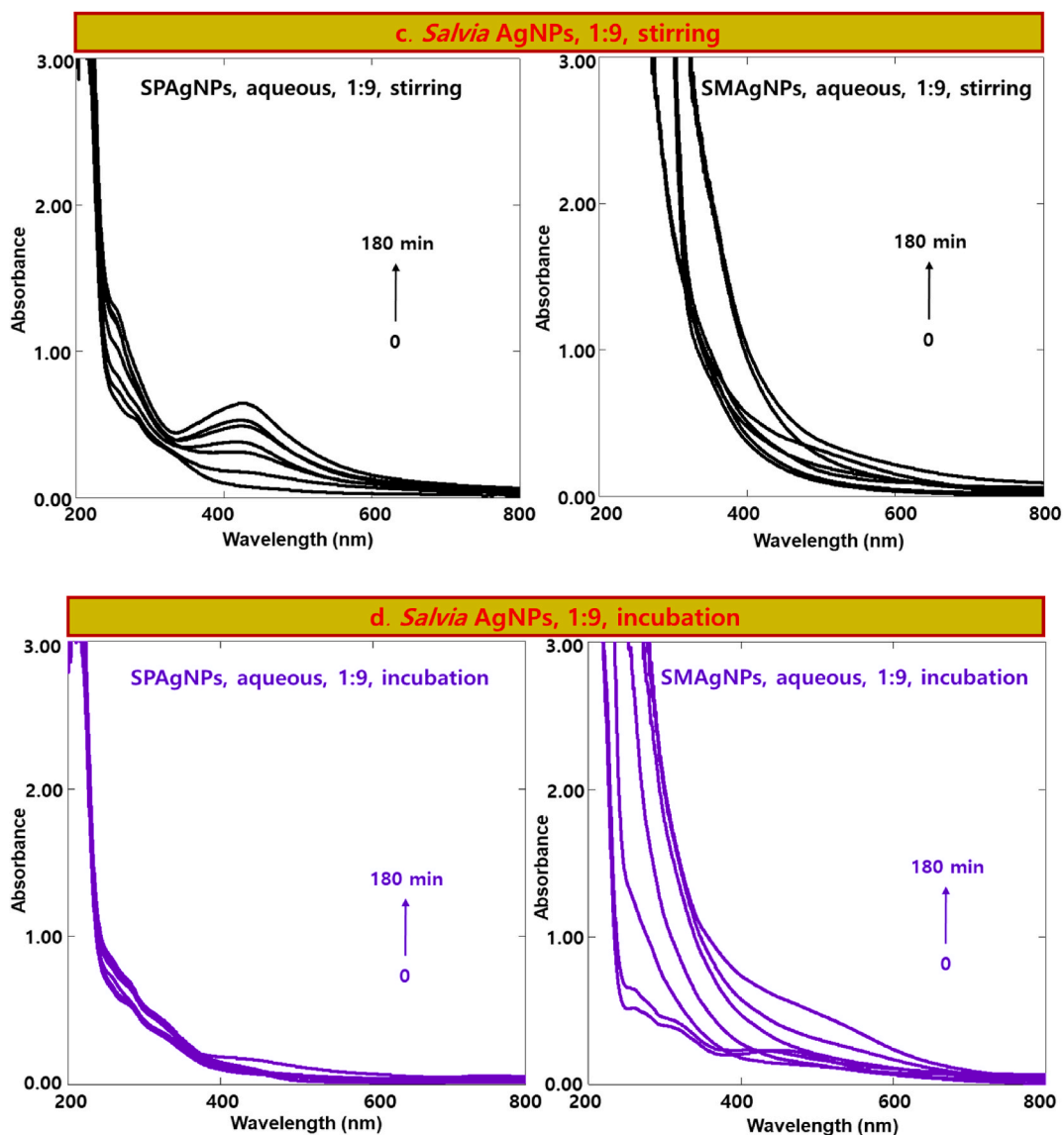


Fig. 1. (continued).

voltages 100V to 30 KV, STEM detector, BSE low and/or high angle, EDS detection range Boron and higher, EDS Quant, line, map, imaging. The SEM analytical parameters were configured as follows: 15 kV accelerating voltage, 0 V deceleration Voltage, x2.0k magnification, 7.7 mm working distance, 4.70 $\mu$ A emission current, and a high lens mode. TEM analysis was conducted on Phillips CM12 (Eindhoven, Netherlands) operating at 120 kV. The samples were stained using uranyl acetate and placed on copper grid to be examined using TEM.

### 2.3. Preparation of *S. plebeia* and *S. moorcroftiana* extracts

*Salvia* aqueous and ethanol extracts were prepared by extracting 10.0 g of powdered samples in 100 mL of solvents (ethanol and water) at 40 °C for 1 h using an ultrasonic bath. The extracts were filtered and utilized in AgNPs synthesis. For assessing the practical application of AgNPs as catalysts in dyes degradation, dyes were extracted from yums, candies, and snack samples (Fig. S2, supplementary material). Briefly, a 10.0 g of sample was extracted with 50 mL of 70 % ethanol solvent containing 2 % ammonia (NH<sub>3</sub>) solution and sonicated using ultrasonic bath at a temperature of 40–45 °C for 1 h. The solutions were left to rest to settle down the starch and sugars in the samples and then the coloured solutions were filtered and concentrated using rotary evaporator at 40 °C and 200 atmospheric pressure. The residual content were then diluted with glacial acetic acid solution (30 mL) for further spectrophotometric analysis [24,25].

## 2.4. Synthesis and characterization of AgNPs

Stable AgNPs were synthesized by treating aqueous and ethanol extracts (reducing/stabilizing/capping agents) of *Salvia* species with silver nitrate solution (silver ion concentrations) in various ratios (1:1 to 1:20) under stirring, sunlight, incubation, and heating at time intervals of 0–180 min (Fig. S3, supplementary material). Preliminary, synthesis of AgNPs was visually observed for colourimetric changes (yellow to dark brown) and then further characterized by appearance of surface Plasmon resonance (SPR) peak observed in 420–440 nm in UV–vis spectroscopic analysis (200–800 nm). After being confirmed, the reaction mixtures were centrifuged and washed with deionized water [26–28]. The synthesized AgNPs were further characterized for their size and morphology by SEM and TEM techniques.

## 2.5. Effect of pH, temperature and salt on stability of AgNPs

The effect of pH, temperature, and salt on stability, physicochemical, and biological activities of AgNPs has been studied as per established procedure [29]. AgNPs pH (2–11) were varied with buffer solution. The changes in intrinsic SPR peak at various pH were recorded. The effect of temperature on AgNPs was studied in the range of 30–80 °C. For salt effect, monovalent and divalent salt solutions (1.0 mM, 50 µL) including CaCl<sub>2</sub>, MgCl<sub>2</sub>, KCl, and NaCl were added to AgNPs solutions (3.0 mL). The reaction mixtures were

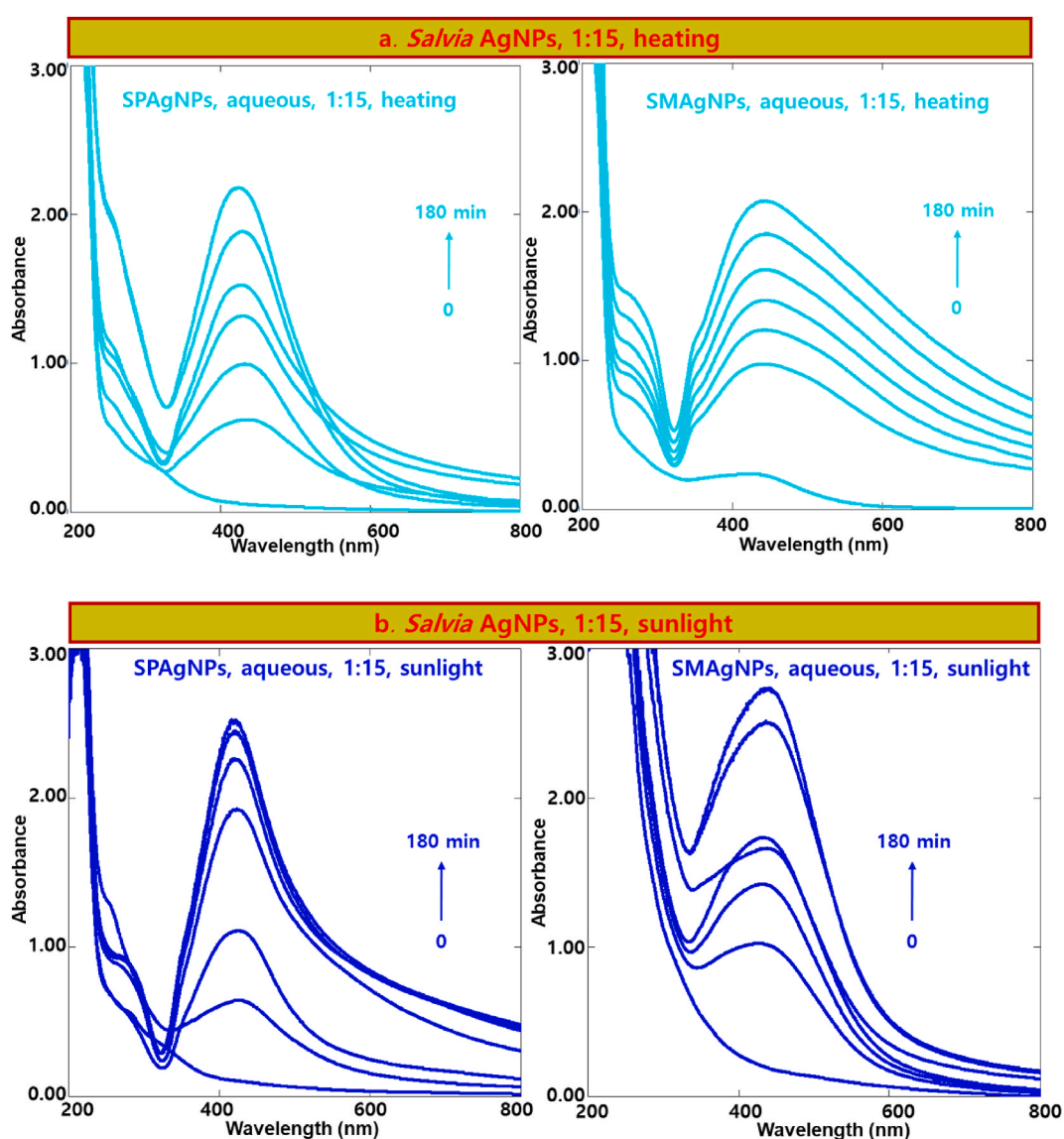


Fig. 2. Successive UV–Vis absorption spectra (200–800 nm) of aqueous extract mediated SPAGNPs and SMAgNPs synthesis in 1:15 under (a) heating (b) sunlight, (c) stirring, and (d) incubation.

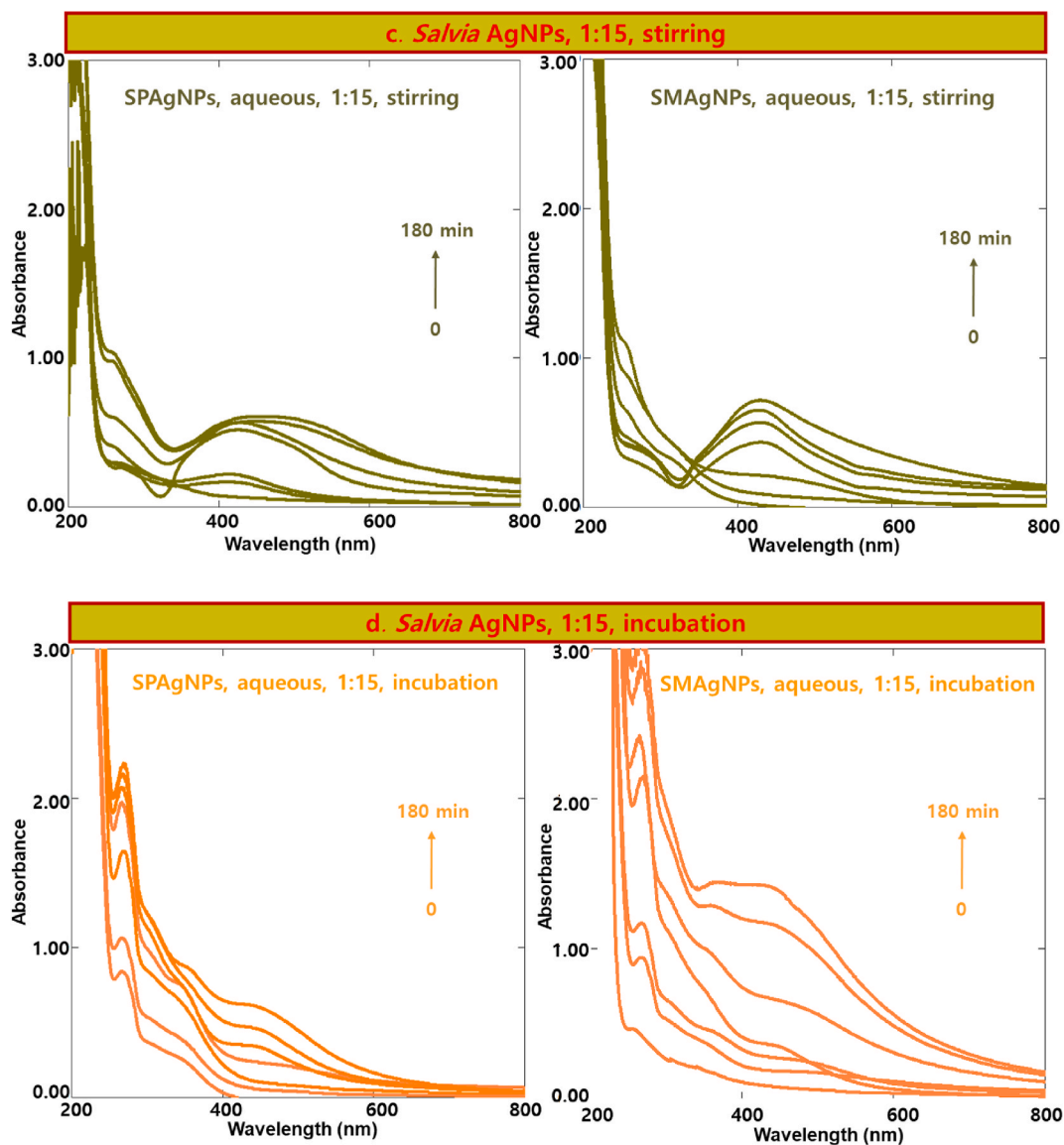


Fig. 2. (continued).

allowed to react in cuvette by shaking for 45–60 s, and then analyzed by UV–vis spectroscopic technique.

## 2.6. Catalytic potential of AgNPs in dyes and antibiotics degradation

To assess AgNPs catalytic activity in dyes degradation, established protocols [26–28] were used. A 2.5 mL (1 mM) of standard/extracted dyes/nitrophenols and 0.5 mL (1 mM) freshly prepared  $\text{NaBH}_4$  were reacted with different dosage (0.1, 0.5, and 1.0 mL) of AgNPs (as catalyst). To assess the catalytic property of AgNPs in real food dyes, the working solutions of extracted dyes were prepared by diluting the stock dye extracts (100  $\mu\text{L}$ ) with ethanol (900  $\mu\text{L}$ ) and water (1000  $\mu\text{L}$ ) to 2.0 mL. The negative and positive controls included the dye solution, and the reaction mixture of dyes/nitrophenols (2.5 mL),  $\text{NaBH}_4$  (0.5 mL) without AgNPs, and deionized water (0.5 mL). Absorbance of the reaction mixtures were recorded at 0 min–180 min and the %decolourization/reduction was calculated from  $(1-A_t/A_0) \times 100$ .

## 2.7. Degradation/reduction of antibiotics by AgNPs

To assess antibiotics degradation by AgNPs as catalyst, a modified procedure [30] was followed. In this assay concentration range (0.001–0.1 mM) of antibiotics, working solutions were prepared in suitable solvents (water, ethanol). A series of experiments on

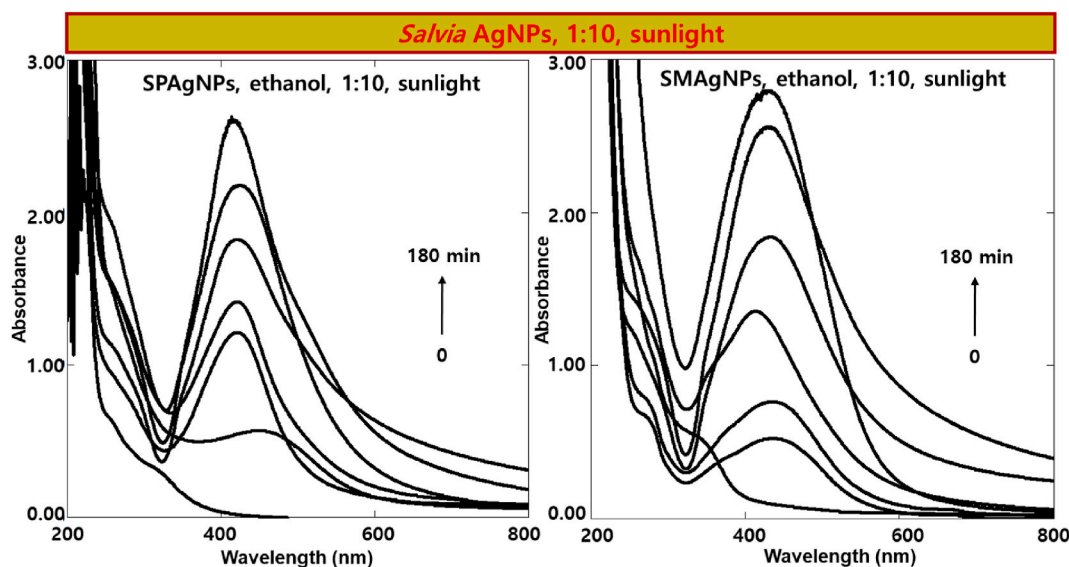


Fig. 3. Successive UV–Vis absorption spectra (200–800 nm) of ethanol extract mediated SPAgNPs and SMAgNPs synthesis in 1:15 under sunlight.

antibiotic solutions, and reaction mixtures [AgNPs (1.0 mL) + NaBH<sub>4</sub> (1.0 mL) + antibiotics (1.0 mL)] were conducted on UV–Vis spectrophotometer from 0 min to 180 min. The negative and positive controls included the antibiotics solution, and the reaction mixture of antibiotics (1.0 mL), NaBH<sub>4</sub> solution (1.0 mL) without AgNPs, and deionized water (1.0 mL). The antibiotics percent reduction (R%) was calculated as  $R\% = (C_0 - C)/C_0 \times 100$  where  $C_0$  is the initial concentration and C represents the final concentration of antibiotics.

### 2.8. Sensing of metals by AgNPs

The sensing capability and applicability of *Salvia* AgNPs was assessed in the detection and recognition of Pb<sup>++</sup>, Cu<sup>++</sup>, Ni<sup>++</sup>, Fe<sup>+++</sup>, and Zn<sup>++</sup> ions following published procedure [31]. Briefly, 1.0 mL of various concentrations (0.01 mM–0.1 mM) of the subject metal ion solutions (spiked samples) were mixed with 2.0 mL of AgNPs. The absorbance were recorded at time intervals of 0 min and 30 min. In addition, the practicality of this sensing ability of AgNPs was tested by considering real Kabul river water samples.

### 2.9. Antioxidant activity of AgNPs

Antioxidant/antiDPPH activity of *Salvia* AgNPs was assessed by DPPH radical inhibition assay [26–28,31]. In this assay, 2500  $\mu$ L of a DPPH solution and 150  $\mu$ L of AgNPs were reacted overnight in dark. A standard (gallic acid) external calibration curve was prepared at 1 mg/mL to 0.01 mg/mL. Samples and controls (negative and positive) including [DPPH (2.5 mL) + solvent (0.15 mL)], and solvent only were also measured alongside the samples at 515 nm. The inhibition percentage (%inhibition) was calculated by a formula  $[(1 - (A_{\text{sample}}/A_{\text{control}}))] \times 100$ , where  $A_{\text{sample}}$  and  $A_{\text{control}}$  denote the absorbance of samples and the controls, respectively. IC<sub>50</sub> values (mg/mL) were calculated using nonlinear regression in GraphPad Prism software.

### 2.10. Antimicrobial activity of AgNPs

Antibacterial activity was evaluated by modified agar well diffusion method against bacterial and fungal/molds strains following the established procedures [26–28]. Fungal strains consisted of *Aspergillus flavus* (plant pathogen) and *Candida albicans* (yeast, ATCC 10231). For agar-well diffusion assay, streaking of fresh overnight culture of each pathogen over Brain heart infusion (BHI) agar plate was done. The plates were incubated at 37 °C for 16 h. Under aseptic conditions, pure isolated colonies were transferred to sterile normal saline (0.85 %) solution and each microbial suspension was adjusted equal to 0.5 McFarland standard. Thereafter, 100  $\mu$ L of the bacterial inoculum of each bacterial strain was spread over pre-solidified Muller Hinton Agar (MHA) plates and 8–9 mm wells were made using a sterile borer. A 100  $\mu$ L of extracts/AgNPs (1 mg/mL) was poured into each of the wells. The plates were incubated for 24 h at 37 °C. Fungal strains were inoculated on Potato Dextrose Agar (PDA) media in order to fresh the strains and incubated for seven days at 27 °C. After seven days, mature growth was observed, then, suspensions of strains were prepared in distilled water 10<sup>4</sup>–10<sup>6</sup> conidia/mL. Thereafter, 100  $\mu$ L of the fungal inoculum of each fungal specie was spread over pre-solidified SDA (Sabouraud Dextrose Agar) plates and 8–9 mm wells were made using a sterile borer. A 100  $\mu$ L of extracts/AgNPs (1 mg/mL) were poured into each of the wells. In order to diffuse it in agar, the plates were incubated for 72 h at 27 °C. Positive control for antifungal activity was nystatin (nilstat) whereas for antibacterial activity, it was broad spectrum antibiotic levofloxacin disc. Dimethyl sulfoxide (DMSO) was used as

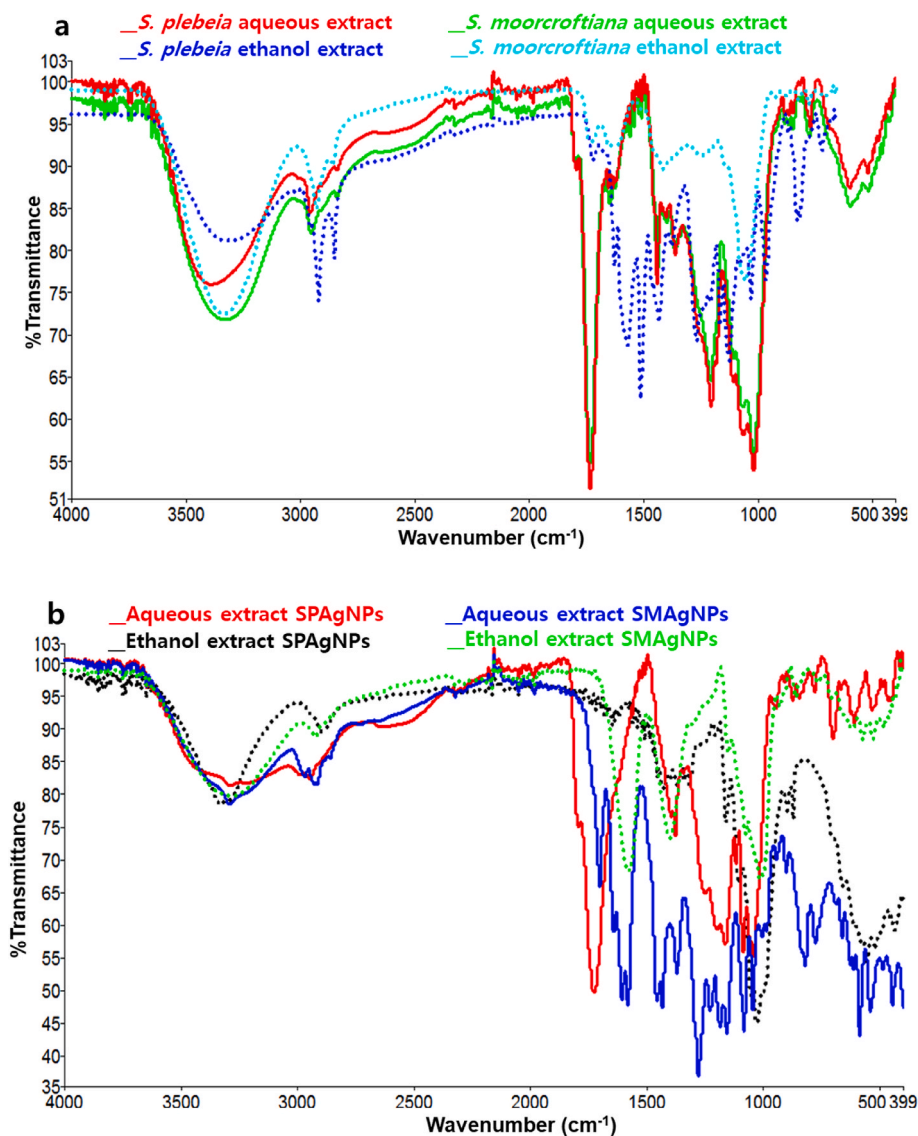


Fig. 4. FT-IR spectra of (a) *S. plebeia* and *S. moorcroftiana* aqueous and ethanol extracts, and (b) aqueous and ethanol extracts mediated SPAgNPs and SMAgNPs.

a negative control. Antimicrobial activity indicated by the zone of inhibition (ZOI) surrounding the well was recorded using a zone scale and represented in millimeter (mm).

### 2.11. Statistical analysis

All the data of antimicrobial and antioxidant activities were represented as means of three replicates ( $n = 3$ ). The differences between the assayed values were analyzed by one-way analysis of variance (ANOVA), followed by Tukey's HSD Test in SPSS software, version 19.0. The IC<sub>50</sub> values in antioxidant activity were calculated using GraphPad Prism 7.0.

## 3. Results and discussion

### 3.1. Synthesis of salvia mediated AgNPs

*Salvia* AgNPs were synthesized using its aqueous and ethanol extracts in a range of ratios under heating, incubation, sunlight, and stirring (Fig. S3, supplementary material). The AgNPs synthesis was primarily confirmed by a colour change and then by a UV-Vis spectroscopic analysis scanned in the wavelength range of 200–800 nm. AgNPs synthesizing from aqueous extract at various quantity

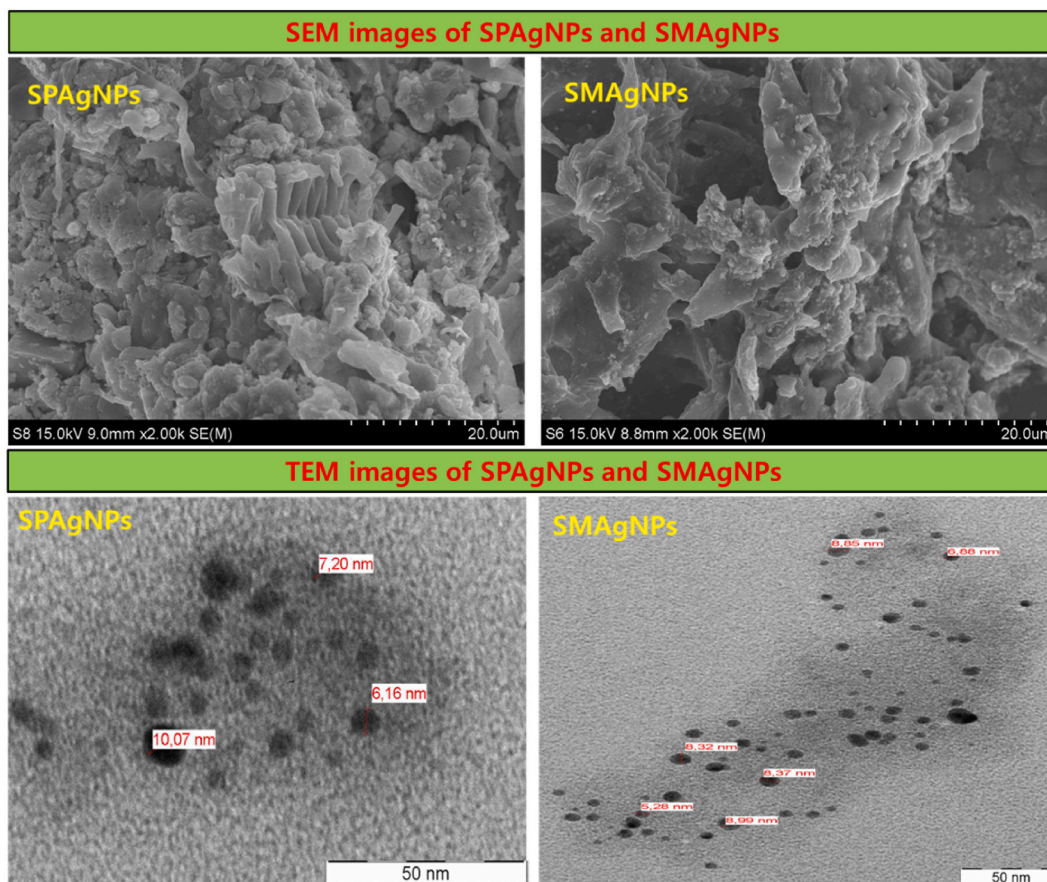


Fig. 5. (a) Surface morphology by SEM and (b) size by TEM techniques of the synthesized SPAgNPs and SMAgNPs.

(1:1 to 1:20), the ratios from 1:1 to 1:5 did not yield AgNPs at all (Fig. S4, supplementary material). However, in 1:9 vol, the colour of the reaction mixture changed from bright yellow to dark brown while synthesizing AgNPs at heating. In UV-Vis spectroscopic analysis, a mixture displayed a significant surface plasmon resonance (SPR) band in 400–430 nm (Fig. 1a). However, at sunlight, stirring, and incubation, no AgNPs were produced (Fig. 1b–d). Furthermore, a 1:15 ratio resulted in the rapid synthesis of AgNPs under heating and sunlight (Fig. 2a and b), whereas stirring or incubation did not generate any significant AgNPs (Fig. 2c and d). Proceeding synthesis with ethanol extract, the best and prominent AgNPs were produced in sunlight with 1:10 proportion (Fig. 3). The results revealed that the phytoconstituents present in *Salvia* extracts successfully reduced/stabilized the  $\text{Ag}^+$  ions to  $\text{Ag}^0$  metal, indicated by SPR absorption band (400–430 nm) of the conducting electrons of Ag metal. The AgNPs synthesis was found dependent on the addition of a reducing agent (*Salvia* extract) in  $\text{AgNO}_3$  solution, which resulted in a colourimetric change from pale yellow to reddish-brown. However, increase in the quantity of reducing agent led to the rapid AgNPs synthesis and eventually agglomeration, which is depicted from the noisy and bathochromic SPR band [28,32].

### 3.2. Characterization of *salvia* mediated AgNPs

To determine and confirm the involvement of functional groups of the phytoconstituents present in the extracts, sizes, and morphology of the synthesized AgNPs, FT-IR, SEM, and TEM spectroscopic and microscopic techniques were used. The FTIR spectra (Fig. 4a) of extracts have shown frequencies/peaks observed at  $3400\text{--}3200\text{ cm}^{-1}$ ,  $3000\text{--}2900\text{ cm}^{-1}$ , and  $1750\text{--}1600\text{ cm}^{-1}$ , which indicated stretching mode of  $\text{--O--H}$ ,  $\text{--C--H}$ , and  $\text{--C--O}$ . An absorption peak at  $2361\text{ cm}^{-1}$  is assigned to  $\text{--C--H}$  stretching of  $\text{--CH}_2$  group. The other absorption frequencies at  $1380\text{--}1350\text{ cm}^{-1}$  ( $\text{--C--O}$  stretching vibrations) and  $1100\text{--}1000\text{ cm}^{-1}$  (stretching  $\text{--C--OH}$  bond vibrations) were also observed. On the other hand, FT-IR spectra of AgNPs (Fig. 4b) depicted the distorted absorption frequencies of  $\text{--O--H}$ ,  $\text{--C--H}$ , and  $\text{--C--O}$ , which indicates the involvement of the subject functional groups in AgNPs synthesis. Hence, it can be concluded that the main functional groups in various phytochemicals (polyphenols, triterpenoids, flavonoids, polysaccharides) may act as capping and stabilizing agent and are accountable for bioreduction of  $\text{Ag}^+$  ions to  $\text{Ag}^0$  NPs as described by several researchers [33–35].

The surface morphology and sizes of the AgNPs were examined using FESEM and TEM techniques. The image scans of AgNPs revealed a mixed spherical, cylindrical, and deep hollow type wells morphology (Fig. 5) with partially aggregated form. In addition,

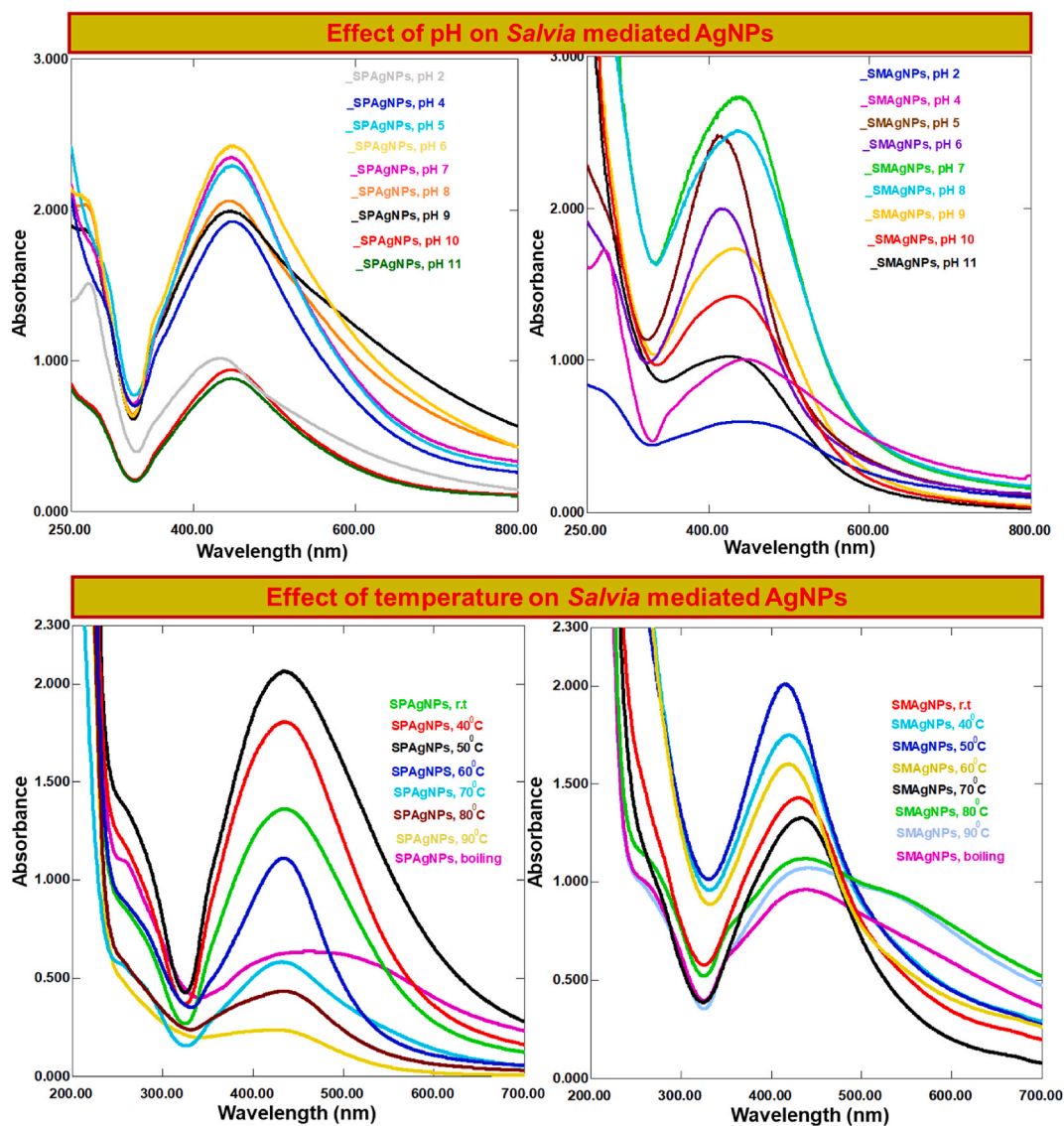


Fig. 6. Successive UV-Vis absorption spectra of effect of pH and temperature on synthesized SPAgNPs and SMAgNPs.

the sizes from TEM analysis were observed as 21.7 nm (SPAgNPs) and 19.9 nm (SMAgNPs). There are number of factors involved in influencing the shape and size of AgNPs such as pH, temperature, and electrostatic force. In this study, it can be concluded that the partial agglomeration may result from the interaction/association of concentrated AgNPs with the phytochemicals such as polysaccharides, proteins, and amino acids [35].

### 3.3. Effect of pH and temperature on stability of AgNPs

The stability of AgNPs is greatly affected by pH and temperature, which ultimately affect the AgNPs size and surface morphology, and hence, the properties. To determine pH and temperature effect on AgNPs, different experiments on pH (2-11) and temperature (ambient to boiling) were conducted. The UV-Visible spectra exhibited that the SPR intensity and  $\lambda_{\max}$  of AgNPs is affected when pH is varied. At pH 4 to 8, AgNPs were stable, whereas decreasing or increasing the pH from the subject range (<4 or >8), the AgNPs get agglomerated and become unstable (Fig. 6). Hence, the results indicate a significant role of pH in reducing silver ions. Several previous studies determining the effect of pH on AgNPs synthesis and stability, claimed that lower pH enhances the NPs nucleation while the higher pH values lead to electrostatic repulsion, causing less NPs synthesis. This reveals that the slightly alkaline pH is favorable for NPs biosynthesis. However, pH values (greater than 9) reduces the NPs synthesis and stability [32,36,37]. Determining temperature effect (r.t, 40 °C, 50 °C, 60 °C, 70 °C, 80 °C, 80 °C, and boiling), the UV-Vis spectral graphs (Fig. 6) depict that increase in the temperature from 40 °C to 60 °C broadens (bathochromic shift) and reduces the intensity of SPR band, which eventually causes rapid

agglomeration. A study of Link & El-Sayed (1999) [38] revealed that to assess a significant effect of temperature on SPR broadening, it must be needed to raise a temperature to hundreds ( $>100\text{ }^{\circ}\text{C}$ ).

### 3.4. Effect of salt on stability of AgNPs

In this analysis, the effect of monovalent and divalent metallic salt solutions including NaCl, KCl,  $\text{MgCl}_2$ , and  $\text{CaCl}_2$  was studied. The UV-vis analysis (Fig. 7a–h) depicts that with increasing salt concentration and the passage of time, sedimentation rate of AgNPs suspension increases. In case of monovalent metallic cations (NaCl and KCl), AgNPs suspended in 0.1 mM NaCl resulted in less sedimentation of AgNPs up to 24 h, and less decrease in absorbance was observed (Fig. 7a–d). However, after 5 days, a considerable decrease in  $\lambda_{\text{max}}$  absorbance and agglomeration occurred. Similarly, AgNPs suspended in 0.1 mM KCl solution, the AgNPs sedimentation rate up to 24 h was lower than that caused due to NaCl salt solution. Regarding divalent salt solutions ( $\text{MgCl}_2$  and  $\text{CaCl}_2$ ), increase in salt concentration, resulted in the immediate colour change (from bright yellow to dark brown) in AgNPs suspension, which resulted in the broadening and bathochromic/red shift of SPR peak (due to agglomeration) (Fig. 7e–h). An increase in divalent cations induces agglomeration of AgNPs due to its interaction/binding with the free/pendant functional groups. From the overall results,  $\text{Ca}^{2+}$  was active in inducing AgNPs agglomeration than  $\text{Mg}^{2+}$ . This might be due to the large size of  $\text{Ca}^{2+}$  ions, which interact with a greater number of AgNPs [39]. The results further suggest that at the same concentration,  $\text{Ca}^{2+}$  plays a slightly more significant role than  $\text{Mg}^{2+}$  in the AgNPs aggregation/agglomeration. In addition, monovalent cations ( $\text{Na}^+$  and  $\text{K}^+$ ) play a small role in AgNPs agglomeration relative to divalent cations.

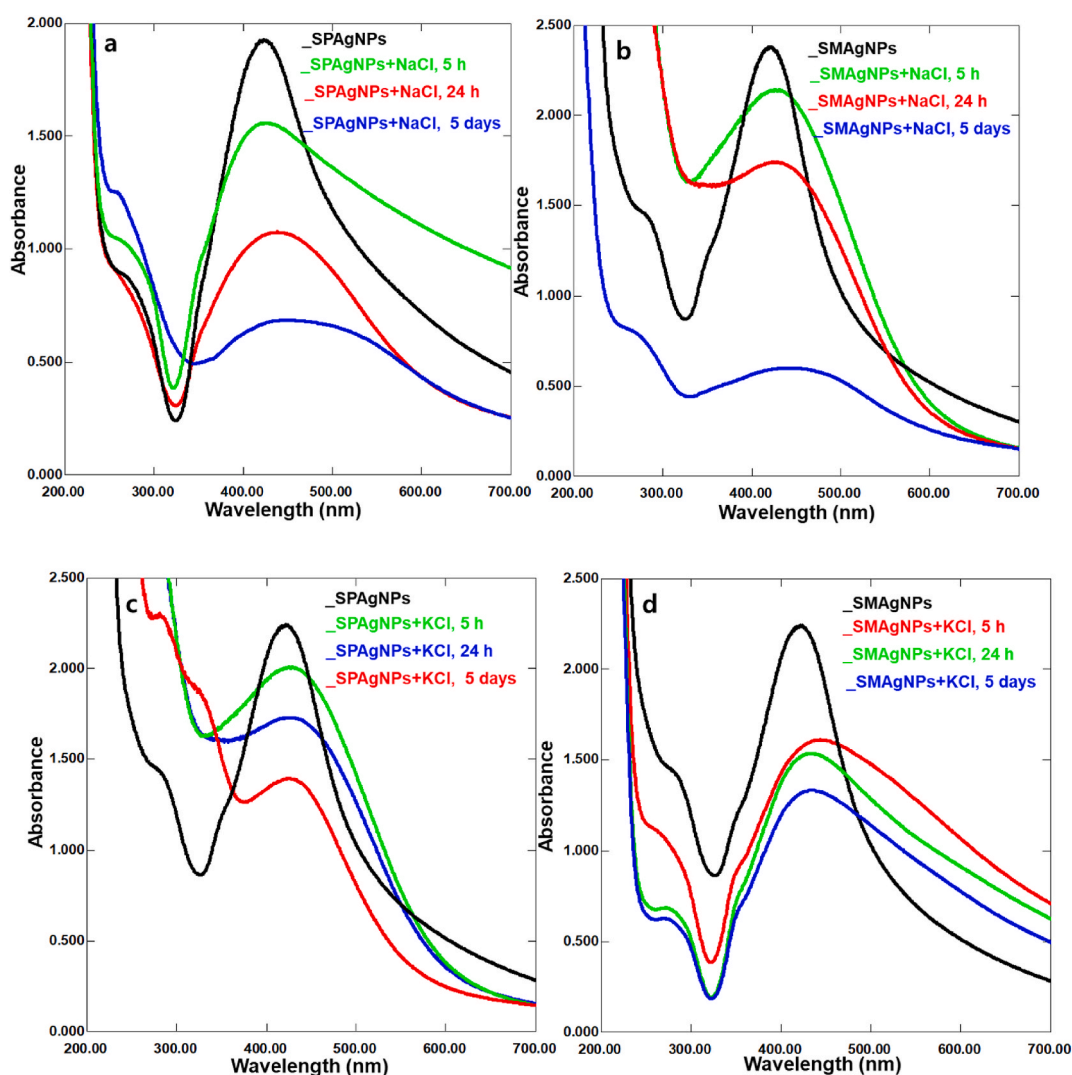


Fig. 7. Successive UV-Vis absorption spectra of effect of salt on synthesized SPAgNPs and SMAgNPs.

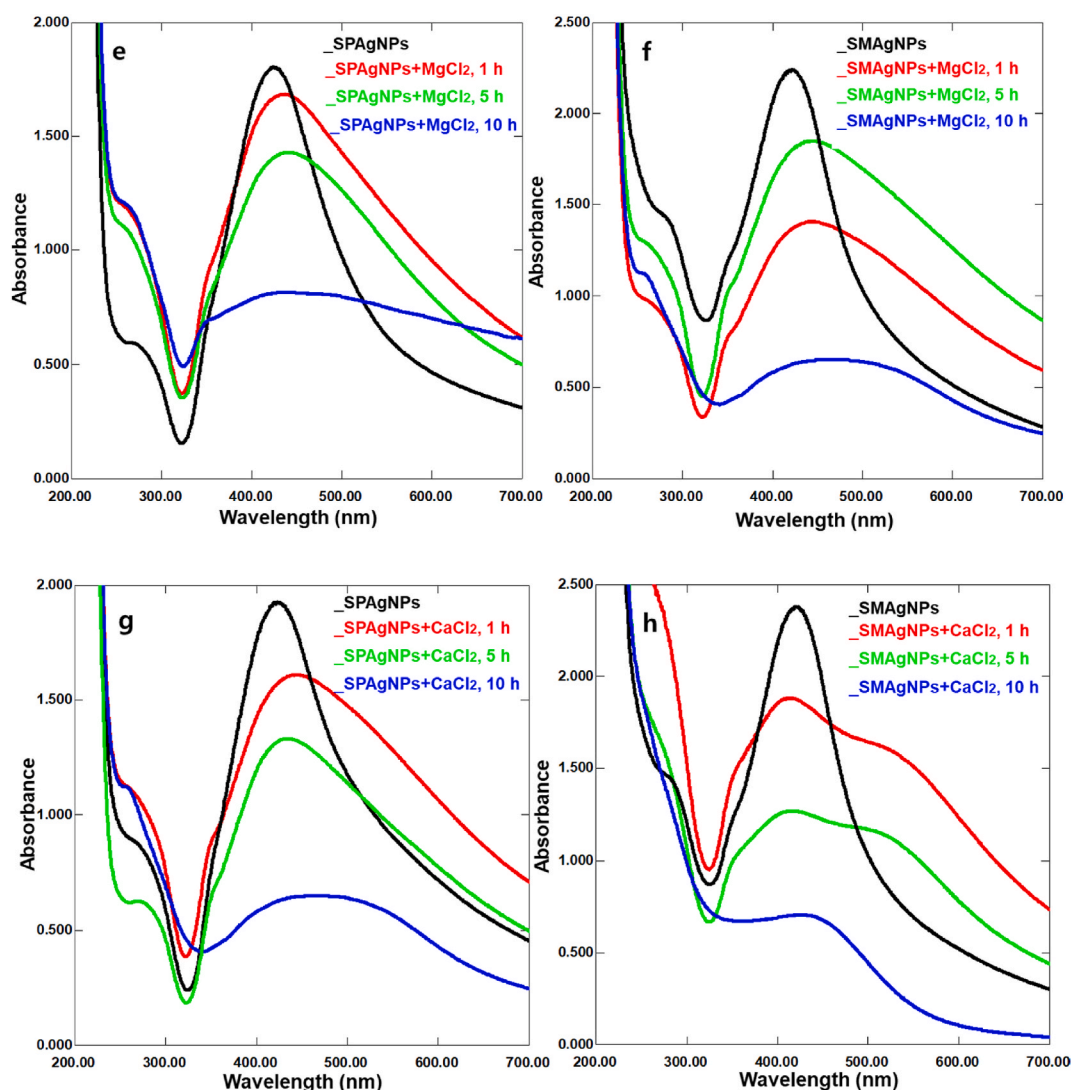
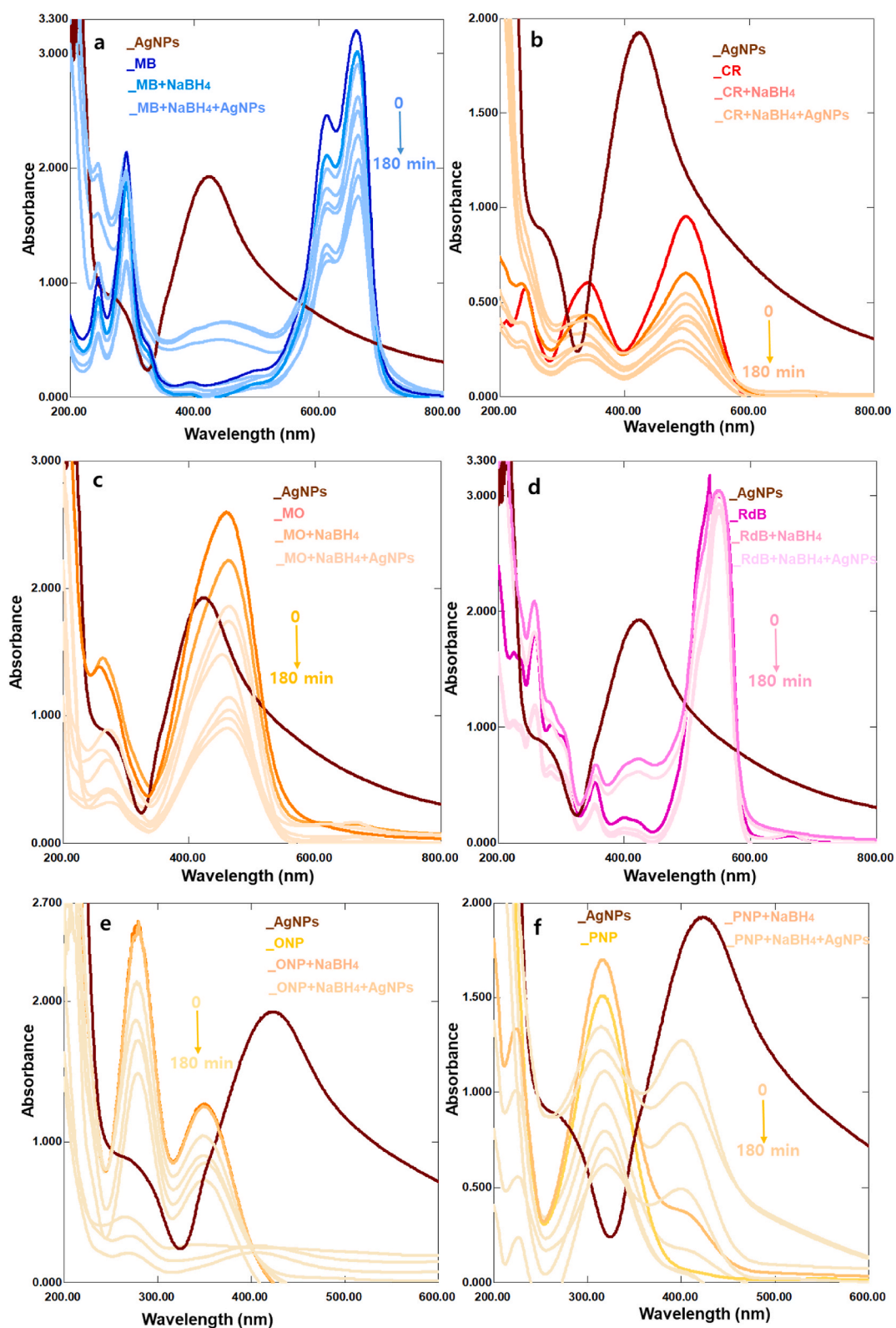


Fig. 7. (continued).

### 3.5. Catalytic potential of salvia AgNPs in dyes degradation

Degradation/reduction of organic dyes can be done in a variety of ways [40]. For instance, the dyes can be degraded to non-toxic species by reducing with  $\text{NaBH}_4$ . However, this reduction is slow process. Hence, there must be some fast and safe techniques to reduce organic dyes. MNPs have interesting catalytic effect in dye reduction. In this reduction process, the activation energy is lowered, which results in less dye being produced. Hence, in order to manage this issue, recently, MNPs was the focus to be used as effective catalysts in degradation of dyes [26–28,41].

The AgNPs synthesized in the current study were used as a catalyst in model dyes reduction. The results (Fig. 8a–f) indicated that the rate of dye degradation is extremely slow in the absence of AgNPs, but upon the addition of AgNPs, the dyes are rapidly reduced over time. This is evident from the related dyes discoloration and decrease in absorption maxima. For example, the catalytic potential of *Salvia* AgNPs against MB (a synthetic cationic thiazine having a prominent peak at 665 nm from  $n-\pi^*$  electronic transition) at different reaction times was investigated. In this analysis, a monotonic decrease in the absorption intensity at 665 nm was observed. The color of MB visually transformed from brilliant blue to colorless. MB dye without AgNPs (control) did not exhibit color change. In an uncatalyzed reaction, the difference in the redox potential of  $\text{NaBH}_4$  and MB did not lead to degradation. Hence, thermodynamically favorable reaction is kinetically unfavourable. A negligible decrease in absorbance of  $\lambda_{\text{max}}$  at 653 nm, 591 nm, and 290 and simultaneous growth at 255 nm was observed after 30 min (Fig. 8a). Mechanism of degradation is supposed to be due to the adsorption of  $\text{BH}_4^-$  ions (donor) and MB (acceptor) on catalyst surface, which carries an electron from  $\text{BH}_4^-$  ions to MB and accelerates the reduction process [42]. The green synthesized AgNPs, which contain phytochemicals as capping agents facilitate electrostatic interactions between catalyst surface and the dye. Hence, a decrease in absorbance, eventually degradation of dye takes place.



**Fig. 8.** Successive UV-Vis absorption spectra for catalytic potential of SPAgNPs and SMAgNPs in (a) MB (b) CR, (c) MO, (d) RdB, (e) ONP, (f) PNP degradation, and (g-j) extracted dyes from yums, candies, and snacks.

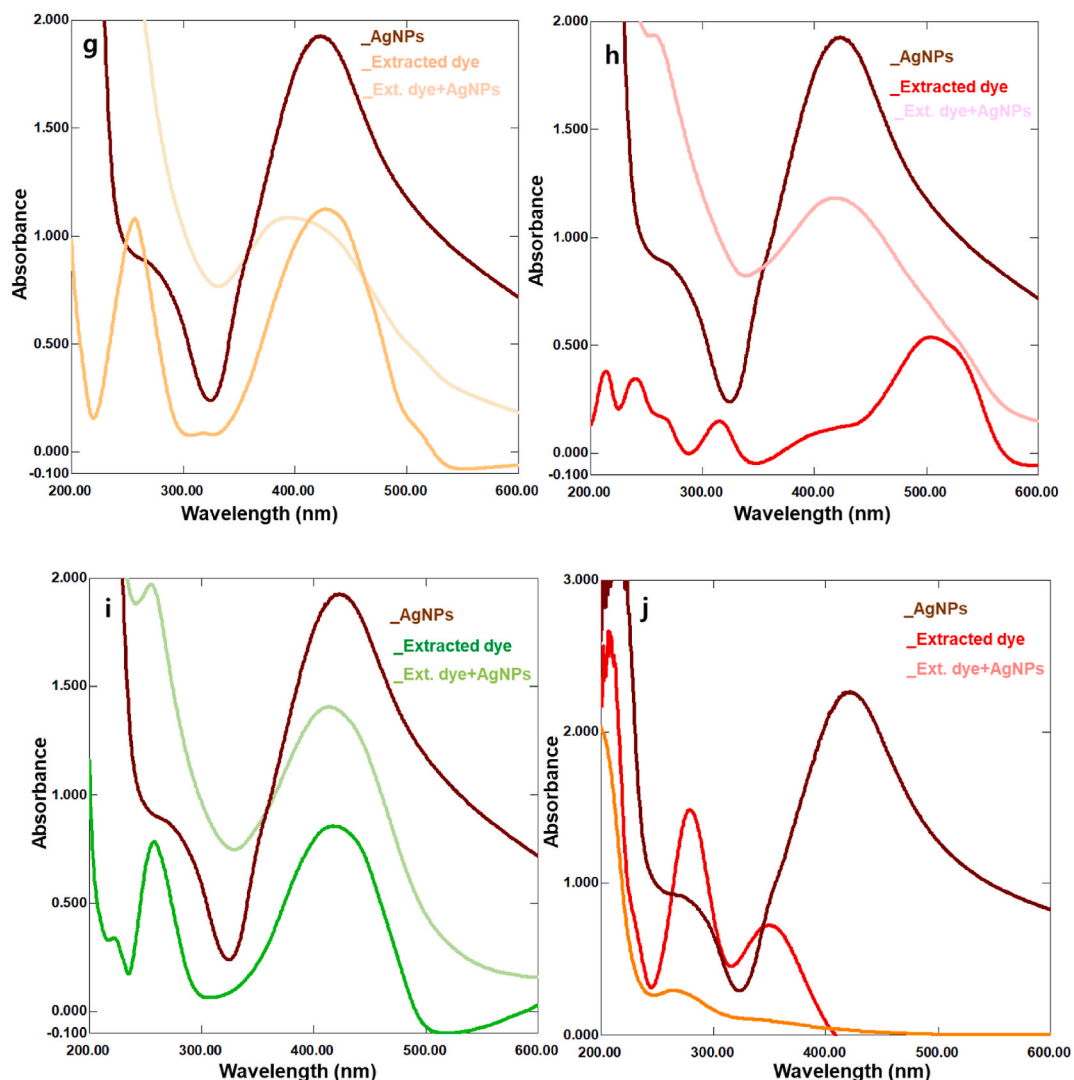


Fig. 8. (continued).

Regarding the CR, MO, and RdB reduction,  $\lambda_{\max}$  at 487 nm (CR), 349 nm (CR), 462 nm (MO), and 550 nm (RdB), AgNPs caused the absorption maxima ( $\lambda_{\max}$ ) of the subject dyes to blue shift (Fig. 8b–d). Furthermore, nitrophenols also exhibited significant degradation (Fig. 8e and f). The overall %degradation/reduction for dyes and nitrophenols was; MB (75 %), CR (85 %), MO (85 %), RdB (<50 %), ONP (95–98 %), and PNP (95–98 %).

The practical application of AgNPs as catalyst in dyes degradation was assessed by the degradation of the colour/dyes extracted from yums, candies, and snacks. From the results of UV–Vis spectral graphs (Fig. 8g–j), it was observed that upon the addition of AgNPs to the extracted dyes causes a decrease in the intensities/absorbance of  $\lambda_{\max}$ , which indicates the degradation. From the study, it was observed that maximum dyes degradation (up to 80–98 %) occurred at 180 min. Above this reaction time, the rate of reaction and efficiency of the catalysts stopped.

### 3.6. Catalytic potential of salvia AgNPs in antibiotics degradation/reduction

Antibiotics degradation was analyzed in the absence and presence of AgNPs respectively. A rich hydrogen source ( $\text{NaBH}_4$ ) was used as a reducing agent and catalyst. From the UV–Vis spectral graphs (Fig. 9), it was noticed that in the absence of AgNPs,  $\text{NaBH}_4$  was unable to reduce antibiotics. Conversely, in the presence of AgNPs, the reduction was very fast and completed within 1–2 h. Levofloxacin (LFX) (Fig. 9) displays an absorption peak at  $\lambda_{\max}$  288 nm, which is reduced upon the AgNPs addition, when the contact time is increased from 0 to 180 min, representing the antibiotics degradation. From the spectral graphs of doxycycline (DXC) (Fig. 9), absorption peaks were at  $\lambda_{\max}$  274 nm and 245 nm, which in the absence of AgNPs undergoes a very small change in absorption up to 24 h. However, upon the addition of AgNPs, degradation became fast and SPR bands got reduced. Amoxicillin (AMX) (Fig. 9) displays

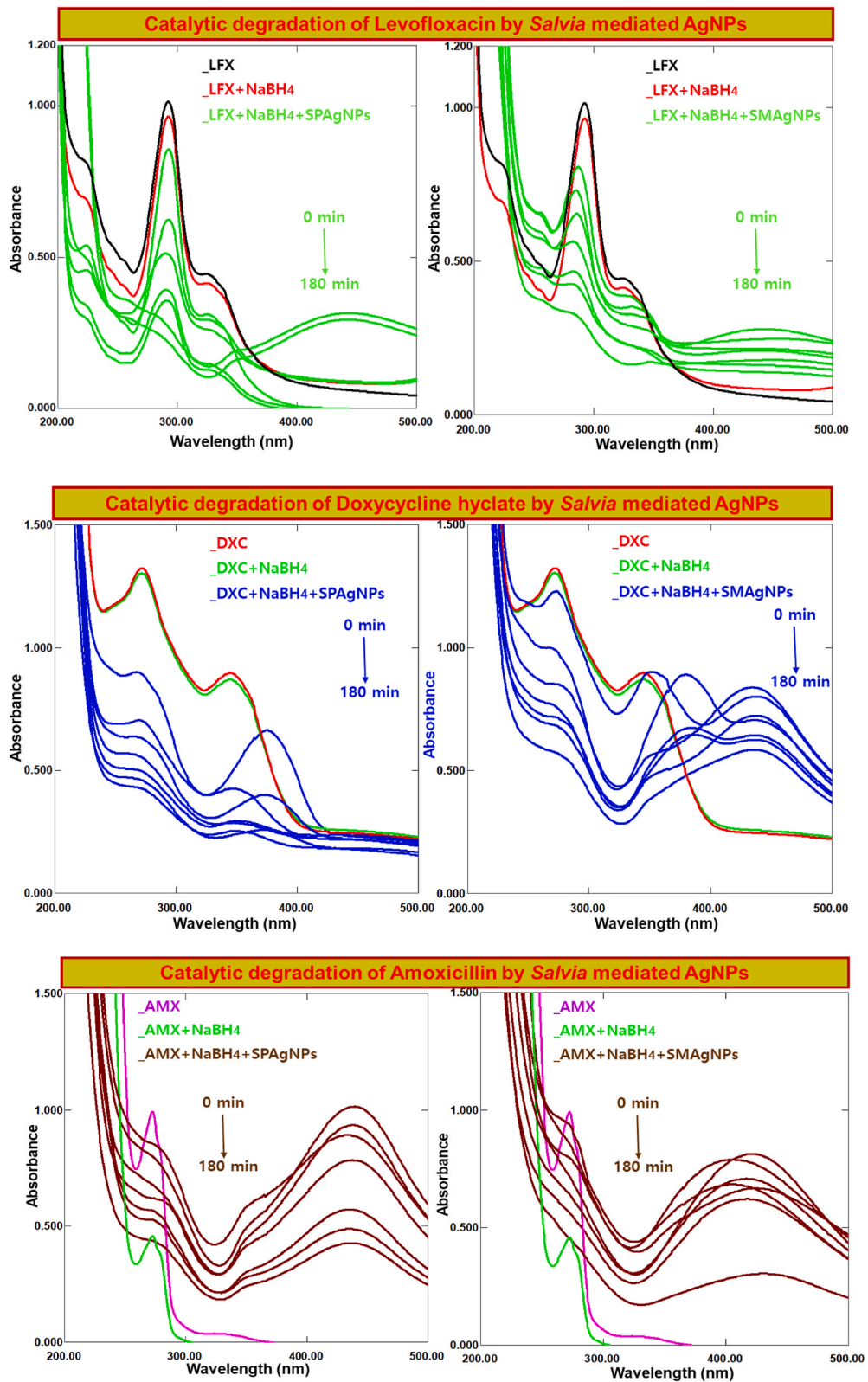
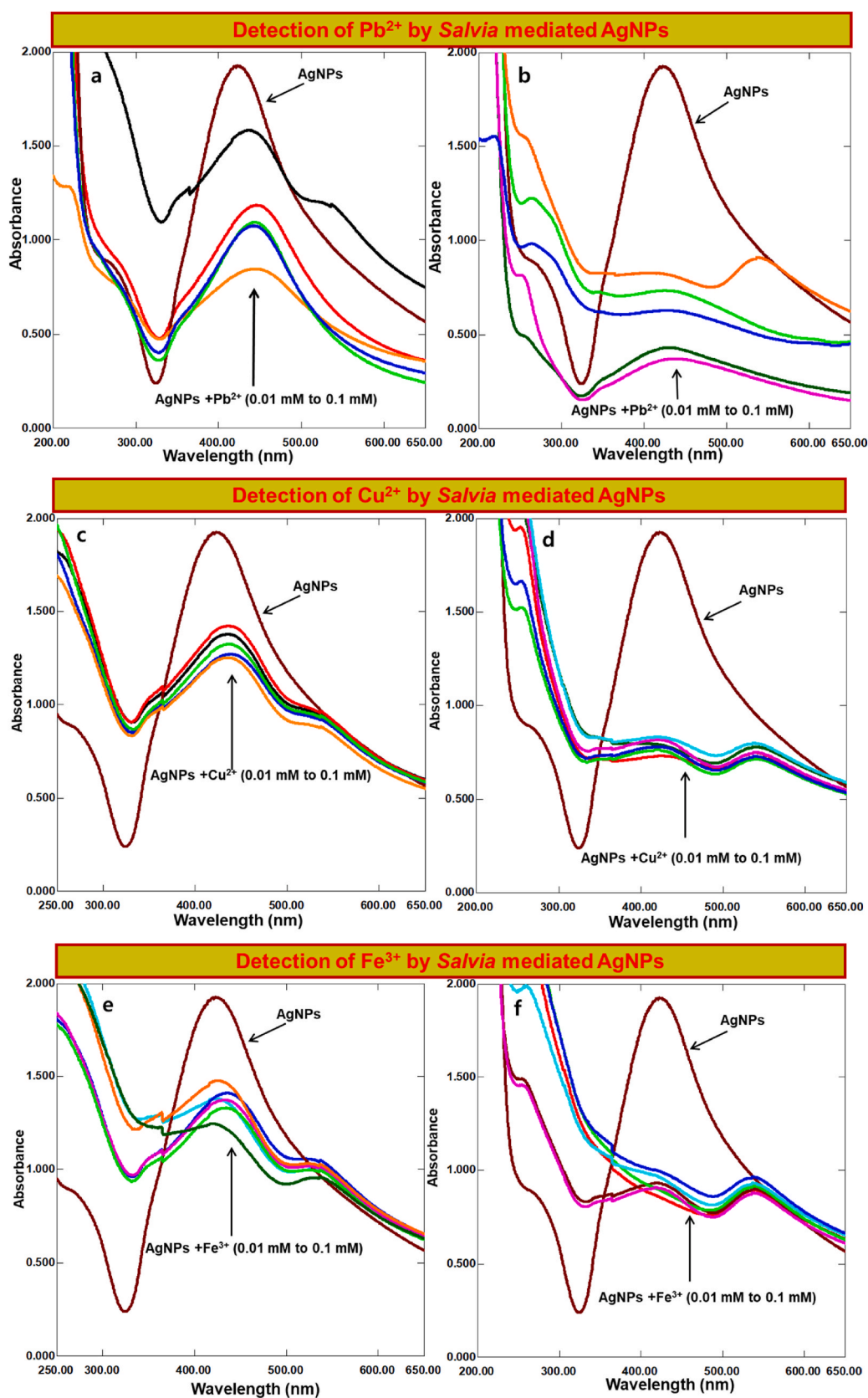


Fig. 9. Successive UV-Vis absorption spectra of degradation of antibiotics; LFX, DXC, and AMX by SPAgNPs and SMAgNPs.



**Fig. 10.** Successive UV-Vis absorption spectra of SPAgNPs and SMAgNPs interaction with different concentrations of metal ion solutions of  $Pb^{+2}$ ,  $Cu^{+2}$ ,  $Fe^{3+}$ ,  $Ni^{+2}$ , and  $Zn^{+2}$  at 0 and 30 min.

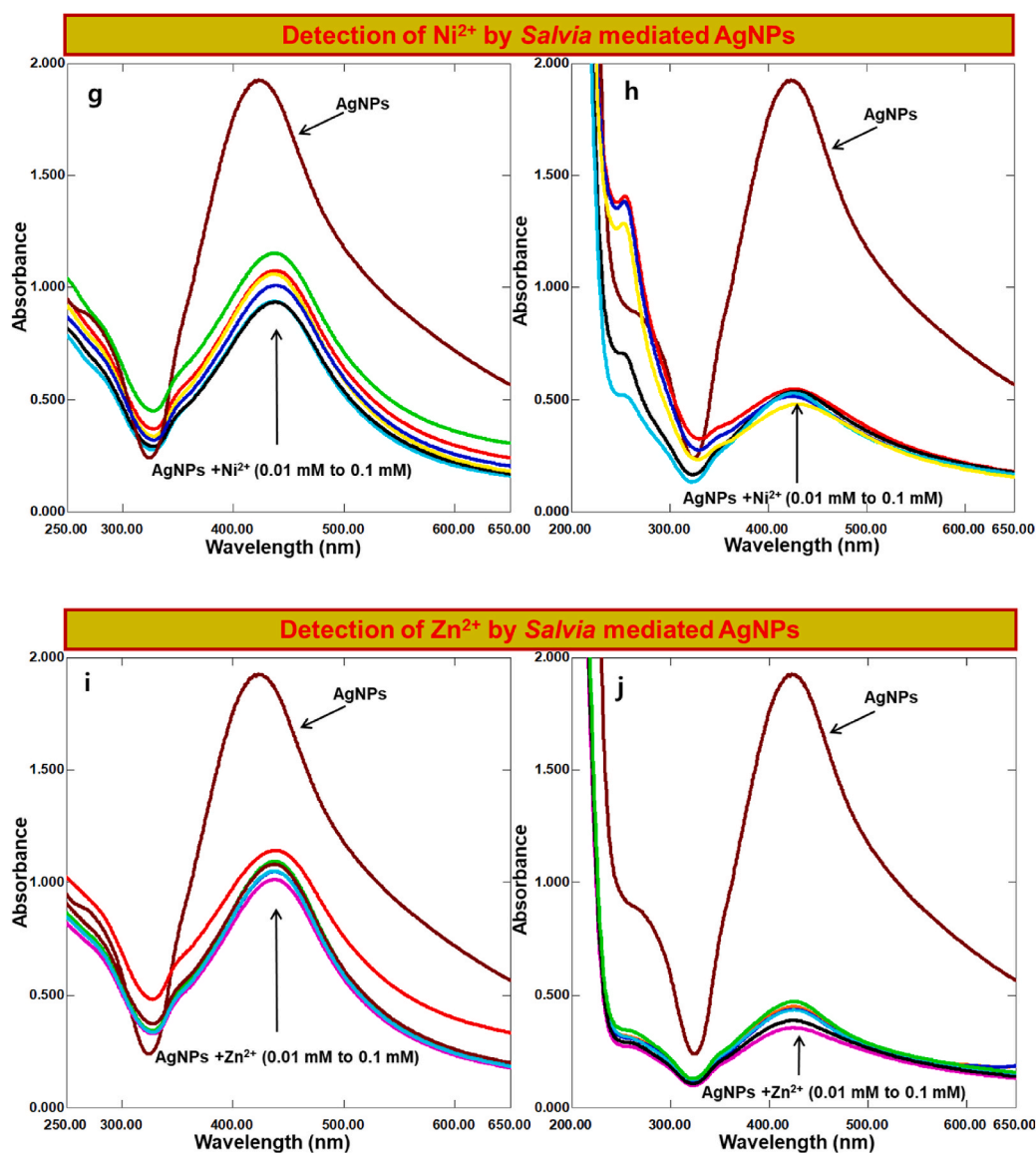


Fig. 10. (continued).

absorption maxima at  $\lambda_{\max}$  229 nm and 278 nm, which upon the addition of AgNPs decreased with the passage of time. From this study, a high catalytic efficiency of the AgNPs can be concluded.

### 3.7. Detection of heavy metals by salvia AgNPs

Nowadays, a wide range of anthropogenic activities causes a rapid influx of heavy metals (arsenic, lead, cadmium, and mercury) into the environment, which ultimately results in environmental (soil, air, and water) toxicity and have negative health impacts. Therefore, it is crucial to remove these contaminants from the environment using safe, effective, and efficient methods. Recently, the use of nanomaterials due to efficient and environmentally benign technique, are the preferred choice for detection and removal of heavy metals as colorimetric sensors.

In the current study, *Salvia* mediated AgNPs was treated with  $\text{Pb}^{2+}$ ,  $\text{Cu}^{2+}$ ,  $\text{Fe}^{3+}$ ,  $\text{Ni}^{2+}$ , and  $\text{Zn}^{2+}$  metal ions. Addition of  $\text{Pb}^{2+}$ ,  $\text{Cu}^{2+}$ , and  $\text{Fe}^{3+}$  solutions caused a significant change in the position and intensity of SPR band when analyzed after 30 min (Fig. 10a–j). The decrease and shifting of SPR band of AgNPs towards bathochromic/red shift indicates agglomeration and destabilization [43,44]. However, upon the addition of  $\text{Ni}^{2+}$  and  $\text{Zn}^{2+}$  ion solutions to AgNPs, there was no significant change in SPR band except a slight decrease in the intensity (Fig. 10g–j). The results revealed that agglomeration by  $\text{Pb}^{2+}$  ions is comparatively higher, which could be attributed to  $\text{Pb}^{2+}$  stronger chelating ability hydroxyl ( $-\text{OH}$ ) and carboxyl ( $-\text{COOH}$ ) groups present on the surface of AgNPs (Fig. 10a

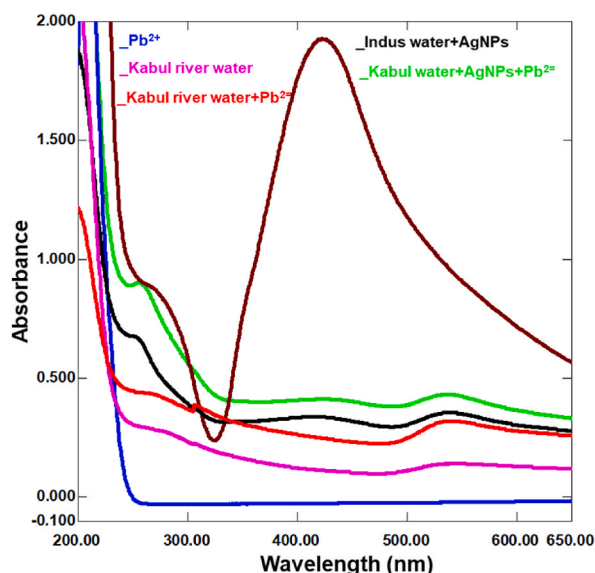


Fig. 11. UV-Vis absorption spectra of SPAgNPs and SMAgNPs interaction with of  $Pb^{+2}$  ion solution in Kabul river water samples.

Table 1

Antioxidant activity of *S. plebeia* and *S. moorcroftiana* aqueous and ethanol extracts and synthesized AgNPs.

Extracts/AgNPs	IC <sub>50</sub> values (mg/mL)	
	<i>S. plebeia</i>	<i>S. moorcroftiana</i>
Ethanol	0.346 ± 0.151 <sup>d</sup>	0.311 ± 0.013 <sup>d</sup>
Aqueous	0.405 ± 0.034 <sup>e</sup>	0.391 ± 0.010 <sup>e</sup>
AgNPs (aqueous)	0.200 ± 0.011 <sup>c</sup>	0.195 ± 0.004 <sup>c</sup>
AgNPs (ethanolic)	0.138 ± 0.008 <sup>b</sup>	0.114 ± 0.003 <sup>b</sup>
Gallic acid (standard)	0.041 ± 0.005 <sup>a</sup>	0.035 ± 0.0006 <sup>a</sup>

Lowercase superscripts (a-e) in a column represent significant differences at  $p < 0.05$ .

Table 2

Antibacterial and antifungal activities of *S. plebeia* and *S. moorcroftiana* aqueous and ethanol extracts and synthesized AgNPs.

Extracts/AgNPs	<i>S. aureus</i>		<i>E. coli</i>	
	<i>S. plebeia</i>	<i>S. moorcroftiana</i>	<i>S. plebeia</i>	<i>S. moorcroftiana</i>
Ethanol extract	11.0–12.0 <sup>b</sup>	12.0–13.0 <sup>b</sup>	8.0–9.0 <sup>a</sup>	8.00–9.00 <sup>a</sup>
Aqueous extract	6.00–7.00 <sup>a</sup>	6.00–7.00 <sup>a</sup>	6.00–7.00 <sup>a</sup>	6.00–7.00 <sup>a</sup>
AgNPs (aqueous)	19.0–20.0 <sup>d</sup>	18.0–19.0 <sup>d</sup>	14.0–15.0 <sup>c</sup>	13.0–14.0 <sup>c</sup>
AgNPs (ethanol)	20.0–21.0 <sup>d</sup>	18.0–19.0 <sup>d</sup>	15.0–16.0 <sup>c</sup>	15.0–16.0 <sup>c</sup>
Vancomycin <sup>a</sup>	19.0–20.0 <sup>d</sup>		12.0–13.0 <sup>b</sup>	
Streptomycin <sup>a</sup>	16.0–17.0 <sup>c</sup>		13.0–14.0 <sup>b</sup>	
<b>Fungal strains</b>				
	<i>Candida albicans</i>		<i>Aspergillus flavus</i>	
	<i>S. plebeia</i>	<i>S. moorcroftiana</i>	<i>S. plebeia</i>	<i>S. moorcroftiana</i>
Ethanol extract	10.0–11.0 <sup>b</sup>	10.0–11.0 <sup>b</sup>	9.00–10.0 <sup>b</sup>	9.00–10.0 <sup>b</sup>
Aqueous extract	7.00–8.00 <sup>a</sup>	7.00–8.00 <sup>a</sup>	6.00–7.00 <sup>a</sup>	6.00–7.00 <sup>a</sup>
AgNPs (aqueous)	19.0–20.0 <sup>c</sup>	19.0–20.0 <sup>c</sup>	18.0–19.0 <sup>c</sup>	18.0–19.0 <sup>c</sup>
AgNPs (ethanol)	20.0–21.0 <sup>c</sup>	20.0–21.0 <sup>c</sup>	20.0–21.0 <sup>d</sup>	20.0–21.0 <sup>d</sup>
Fluconazole <sup>a</sup>	19.0–20.0 <sup>c</sup>		20.0–21.0 <sup>d</sup>	
Amphotericin <sup>a</sup>	19.0–20.0 <sup>c</sup>		19.0–20.0 <sup>c</sup>	

Lowercase superscripts (a-d) in a column represent significant differences at  $p < 0.05$ .

<sup>a</sup> Standards.

&b). The study further depicts that increasing the concentration of  $Pb^{2+}$ ,  $Cu^{2+}$ ,  $Fe^{3+}$ ,  $Ni^{2+}$ , and  $Zn^{2+}$  ion solutions gradually reduces the intensity of SPR band. The practical applicability of the sensing potential of AgNPs was assessed by using real water (Kabul river) samples. The results (Fig. 11) revealed that SPR band of AgNPs vanished when added to the Kabul water samples. Hence, it can be

concludes that the subject AgNPs can be used as sensors to detect toxic heavy metal ions ( $Pb^{2+}$ ) in water samples.

### 3.8. Antioxidant activity of salvia AgNPs

Oxidative stress, a process of generating free radicals by oxidation of DNA, proteins, and lipids, is the root cause of various complications. Plants containing polyphenolic constituents exhibit key antioxidant (due to  $-OH$  group) and antimicrobial properties. Antioxidants are the constituents, which reduce free radicals, and, hence, lower the oxidative stress. In the current study, the synthesized AgNPs were assessed for antioxidant capacity via DPPH assay in which a DPPH $^{\bullet}$  radical (purple colour) gains an electron from an antioxidant constituents, and, hence, reduces to DPPH-H (yellow colour). The results of anti-DPPH potential of *Salvia* AgNPs (Table 1) showed that the ethanol extract mediated AgNPs have excellent inhibition of DPPH and the  $IC_{50}$  values were lower (0.138 mg/mL, SPAgNPs and 0.114 mg/mL, SMAgNPs) than aqueous extract-mediated AgNPs (0.200 mg/mL, SPAgNPs and 0.195 mg/mL, SMAgNPs). This high antioxidative potential of the AgNPs of ethanol extract might be assigned to the abundance of phytochemicals (polyphenols) adhered to the surface of AgNPs.

### 3.9. Antimicrobial activities of salvia AgNPs

Due to morphological characteristics (size and shape), AgNPs play a key role as potential antimicrobial agents against most of the bacterial and fungal strains. The antimicrobial activity of AgNPs is due to the accumulation and formation of “pits and gaps” of AgNPs in microbial cell membrane, and destruction of permeability of cell membrane, which eventually causes cell death. Hence, a variety of microbial strains can be inhibited [45,46]. From the results of antibacterial activity (Table 2), AgNPs were found to be the most active inhibitors of both the microbial (bacterial and fungal) strains. The inhibition zones exhibited by *Salvia* mediated AgNPs are 18.0 mm–21.0 mm against *S. aureus* and 13.0 mm–16.0 mm against *E. coli*. It was observed that even at low concentration of AgNPs, a complete inhibition of Gram-positive strain occurred. This could be due to biomolecules adsorbed on the AgNPs surface. However, against Gram-negative strains, a mild effect was shown by AgNPs. Nowadays, it is essential to develop biocompatible and ecofriendly antifungal agents. AgNPs have been recorded as potential anti-fungal drugs against various fungi. In antifungal activity conducted in this investigation (Table 2), aqueous extract mediated AgNPs exhibited inhibition zones of 19.0–20.0 mm and 18.0–19.0 mm whereas ethanol extract mediated AgNPs have shown inhibition of 20.0–21.0 mm against *C. albicans* and *A. flavus*, respectively.

## 4. Conclusions

The current research work describes *Salvia* mediated AgNPs synthesis under various conditions. The synthesized AgNPs (1:9, 1:10, 1:15) performed excellent catalytic activity in dyes and antibiotics degradation, and sensing ability in heavy metals ( $Pb^{++}$ ) detection in model and real water samples. Based on the key features of less degradation time and good sensing ability of AgNPs, explores its great potential in treating wastewater containing organic dyes, antibiotics, and heavy metals. This research work opens new dimensions for synthesizing cost effective, time effective, environmental friendly, and efficient catalyst, which might provide promising efficiency in the treatment of environmental contaminants (from dyes, antibiotics, and toxic metals).

### Statements and declarations

Authors confirm that the manuscript has been read and approved by all named authors and that there are no other persons who satisfied the criteria for authorship but are not listed. It is further confirmed that the order of authors listed in the manuscript has been approved by all authors. The corresponding author on behalf of all authors of the manuscript further declares that there is no any potential competing interests.

### Data availability statement

The authors confirm that the data supporting the findings of this study are available within the article and its supplementary materials. However, the raw data will be available upon request from the corresponding author.

### CRediT authorship contribution statement

**Sana Ihsan:** Writing – original draft, Investigation. **Hajera Gul:** Writing – review & editing, Writing – original draft. **Nargis Jamila:** Supervision, Funding acquisition, Conceptualization. **Naeem Khan:** Methodology, Conceptualization. **Riaz Ullah:** Resources, Funding acquisition. **Ahmed Bari:** Funding acquisition. **Tan Wen Nee:** Formal analysis. **Joon Ho Hwang:** Formal analysis. **Rehana Masood:** Resources, Investigation.

### Declaration of competing interest

The authors declare the following financial interests/personal relationships which may be considered as potential competing interests: Nargis Jamila reports financial support was provided by Higher Education Commission Pakistan.

## Acknowledgement

Authors wish to thank Researchers Supporting Project Number (RSP2024R110) at King Saud University Riyadh Saudi Arabia for financial support.

## Appendix A. Supplementary data

Supplementary data to this article can be found online at <https://doi.org/10.1016/j.heliyon.2024.e25814>.

## References

- [1] T. Behl, I. Kaur, A. Sehgal, S. Singh, N. Sharma, S. Bhatia, A.A. Harrasi, S. Bungau, The dichotomy of nanotechnology as the cutting edge of agriculture: nano-farming as an asset versus nanotoxicity, *Chemosphere* 288 (2022) 132533, <https://doi.org/10.1016/j.chemosphere.2021.132533>.
- [2] F. Mo, Q. Zhou, Y. He, Nano-Ag: environmental applications and perspectives, *Sci. Total Environ.* 829 (2022) 154644, <https://doi.org/10.1016/j.scitotenv.2022.154644>.
- [3] S. Sahani, Y.C. Sharma, Advancements in applications of nanotechnology in global food industry, *Food Chem.* 342 (2021) 128318, <https://doi.org/10.1016/j.foodchem.2020.128318>.
- [4] S. Gottardo, A. Mech, J. Drbohlavová, A. Malyska, S. Bøwadt, J.R. Sintes, H. Rauscher, Towards safe and sustainable innovation in nanotechnology: state-of-play for smart nanomaterials, *NanoImpact* 21 (2021) 100297, <https://doi.org/10.1016/j.impact.2021.100297>.
- [5] Z.T. Hu, Y. Chen, Y.F. Fei, S.L. Loo, G. Chen, M. Hu, J. Zhao, Y. Zhang, J. Wang, An overview of nanomaterial-based novel disinfection technologies for harmful microorganisms: mechanism, synthesis, devices and application, *Sci. Total Environ.* (2022) 155720, <https://doi.org/10.1016/j.scitotenv.2022.155720>.
- [6] N. Yadav, S.S. Yadav, A.K. Chhillar, J.S. Rana, An overview of nanomaterial based biosensors for detection of Aflatoxin B1 toxicity in foods, *Food Chem. Toxicol.* 152 (2021) 112201, <https://doi.org/10.1016/j.fct.2021.112201>.
- [7] Y. Wang, D. O'Connor, Z. Shen, I.M. Lo, D.C. Tsang, S. Pehkonen, S. Pu, D. Hou, Green synthesis of nanoparticles for the remediation of contaminated waters and soils: constituents, synthesizing methods, and influencing factors, *J. Clean. Prod.* 226 (2019) 540–549, <https://doi.org/10.1016/j.jclepro.2019.04.128>.
- [8] M. Danouche, E.A. Hicham, E.G. Naima, E. Biodegradation of environmental pollutants by marine yeasts, in: *Marine Organisms: A Solution to Environmental Pollution? Uses in Bioremediation and in Biorefinery*, Springer International Publishing, Cham, 2023, pp. 79–91, [https://doi.org/10.1007/978-3-031-17226-7\\_5](https://doi.org/10.1007/978-3-031-17226-7_5).
- [9] M. Danouche, H. El Arroussi, N.D. El Ghachtouli, Mycoremediation of synthetic dyes by yeast cells: a sustainable biodegradation approach, *Environ. Sustain.* 4 (2022) 5–22, <https://doi.org/10.1007/s42398-020-00150-w>.
- [10] M. Danouche, N. El Ghachtouli, A. Aasfar, I. Bennis, H. El Arroussi, Pb (II)-phycoremediation mechanism using *Scenedesmus obliquus*: cells physicochemical properties and metabolomic profiling, *Heliyon* 8 (2022) e08967, <https://doi.org/10.1016/j.heliyon.2022.e08967>.
- [11] F. Behzad, S.M. Naghib, S.N. Tabatabaei, Y. Zare, K.Y. Rhee, An overview of the plant-mediated green synthesis of noble metal nanoparticles for antibacterial applications, *J. Ind. Eng. Chem.* 94 (2021) 92–104, <https://doi.org/10.1016/j.jiec.2020.12.005>.
- [12] N. Rajana, A. Mounika, P.S. Chary, V. Bhavana, A. Urati, D. Khatri, S.B. Singh, N.K. Mehra, Multifunctional hybrid nanoparticles in diagnosis and therapy of breast cancer, *J. Contr. Release* 352 (2022) 1024–1047, <https://doi.org/10.1016/j.jconrel.2022.11.009>.
- [13] A. Yadav, H. Kumar, R. Shrama, R. Kumari, Synthesis, processing, and applications of 2D (nano) materials: a sustainable approach, *Surface. Interfac.* (2023) 102925, <https://doi.org/10.1016/j.surfin.2023.102925>.
- [14] N. Al-Qasbi, W. Al-Gethami, D. Saleh, A. Abuziad, A sustainable approach for the synthesis of metallic nanoparticles and its application as antimicrobial agents, *J. Mater. Res. Technol.* 9 (2020) 13036–13042, <https://doi.org/10.1016/j.jmrt.2020.09.053>.
- [15] A.K. Shukla, S. Iravani, Metallic nanoparticles: green synthesis and spectroscopic characterization, *Environ. Chem. Lett.* 15 (2017) 223–231, <https://doi.org/10.1007/s10311-017-0618-2>.
- [16] M. Sooraj, A.S. Nair, D. Vineetha, Sunlight-mediated green synthesis of silver nanoparticles using *Sida retusa* leaf extract and assessment of its antimicrobial and catalytic activities, *Chem. Pap.* 75 (2021) 351–363, <https://doi.org/10.1007/s11696-020-01304-0>.
- [17] X.-F. Zhang, Z.-G. Liu, W. Shen, S. Gurunathan, Silver nanoparticles: synthesis, characterization, properties, applications, and therapeutic approaches, *Int. J. Mol. Sci.* 17 (2016) 1534, <https://doi.org/10.3390/ijms17091534>.
- [18] K. Chand, D. Cao, D.E. Fouad, A.H. Shah, A.Q. Dayo, K. Zhu, M.N. Lakhan, G. Mehdi, S. Dong, Green synthesis, characterization and photocatalytic application of silver nanoparticles synthesized by various plant extracts, *Arab. J. Chem.* 13 (2020) 8248–8261, <https://doi.org/10.1016/j.arabjc.2020.01.009>.
- [19] E. Wanarska, I. Maliszewska, The possible mechanism of the formation of silver nanoparticles by *Penicillium cycloptium*, *Bioorg. Chem.* 93 (2019) 102803, <https://doi.org/10.1016/j.bioorg.2019.02.028>.
- [20] M.A. Islam, M.V. Jacob, E. Antunes, A critical review on silver nanoparticles: from synthesis and applications to its mitigation through low-cost adsorption by biochar, *J. Environ. Manag.* 281 (2021) 111918, <https://doi.org/10.1016/j.jenvman.2020.111918>.
- [21] Y.Y. Liang, X.H. Wan, F.J. Niu, S.M. Xie, H. Guo, Y.Y. Yang, L.Y. Guo, C.Z. Zhou, *Salvia plebeia* R. Br.: an overview about its traditional uses, chemical constituents, pharmacology and modern applications, *Biomed. Pharmacother.* 121 (2022) 109589, <https://doi.org/10.1016/j.biopha.2019.109589>.
- [22] P. Nhoek, H.S. Chae, Y.M. Kim, P. Pel, J. Huh, H.W. Kim, Y.H. Choi, K. Lee, Y.W. Chin, Sesquiterpenoids from the aerial parts of *Salvia plebeia* with inhibitory activities on proprotein convertase subtilisin/kexin type 9 expression, *J. Nat. Prod.* 84 (2021) 220–229, <https://doi.org/10.1021/acs.jnatprod.0c00829>.
- [23] M. Zahid, O. Ishrud, Y. Pan, M. Asim, M. Riaz, V.U. Ahmad, Flavonoid glycosides from *Salvia moorcroftiana* wall, *Carbohydr. Res.* 337 (2002) 403–407, [https://doi.org/10.1016/S0008-6215\(02\)00008-3](https://doi.org/10.1016/S0008-6215(02)00008-3).
- [24] I.M. Yusoff, Z.M. Taher, Z. Rahmat, L.S. Chua, A review of ultrasound-assisted extraction for plant bioactive compounds: phenolics, flavonoids, thymols, saponins and proteins, *Food Res. Int.* 157 (2022) 111268, <https://doi.org/10.1016/j.foodres.2022.111268>.
- [25] N. Echegaray, N. Guzel, M. Kumar, M. Guzel, A. Hassoun, J.M. Lorenzo, Recent advancements in natural colorants and their application as coloring in food and in intelligent food packaging, *Food Chem.* 404 (2023) 134453, <https://doi.org/10.1016/j.foodchem.2022.134453>.
- [26] N. Jamila, N. Khan, A. Bibi, A. Haider, S.N. Khan, A. Atlas, U. Nishan, A. Minhaz, F. Javed, A. Bibi, *Piper longum* catkin extract mediated synthesis of Ag, Cu, and Ni nanoparticles and their applications as biological and environmental remediation agents, *Arab. J. Chem.* 13 (2020) 6425–6436, <https://doi.org/10.1016/j.arabjc.2020.06.001>.
- [27] N. Jamila, N. Khan, I.M. Hwang, M. Saba, F. Khan, F. Amin, S.N. Khan, A. Atlas, F. Javed, A. Minhaz, Characterization of natural gums via elemental and chemometric analyses, synthesis of silver nanoparticles, and biological and catalytic applications, *Int. J. Biol. Macromol.* 147 (2020) 853–866, <https://doi.org/10.1016/j.ijbiomac.2019.09.245>.
- [28] W. Khan, N. Khan, N. Jamila, R. Masood, A. Minhaz, F. Amin, A. Atlas, U. Nishan, Antioxidant, antibacterial, and catalytic performance of biosynthesized silver nanoparticles of *Rhus javanica*, *Rumex hastatus*, and *Callistemon viminalis*, *Saudi J. Biol. Sci.* 29 (2022) 894–904, <https://doi.org/10.1016/j.sjbs.2021.10.016>.
- [29] A. Anwar, A. Minhaz, N.A. Khan, K. Kalantari, A.B.M. Afifi, M.R. Shah, Synthesis of gold nanoparticles stabilized by a pyrazinium thioacetate ligand: a new colorimetric nanosensor for detection of heavy metal Pd (II), *Sens. Actuators B Chem.* 257 (2018) 875–881, <https://doi.org/10.1016/j.snb.2017.11.040>.

- [30] T. Makropoulou, I. Kortidis, K. Davididou, D.E. Motaung, E. Chatzisyneon, Photocatalytic facile ZnO nanostructures for the elimination of the antibiotic sulfamethoxazole in water, *J. Water Process Eng.* 36 (2020) 101299, <https://doi.org/10.1016/j.jwpe.2020.101299>.
- [31] N. Jamila, N. Khan, N. Bibi, M. Waqas, S.N. Khan, A. Atlas, F. Amin, F. Khan, M. Saba, Hg (II) sensing, catalytic, antioxidant, antimicrobial, and anticancer potential of *Garcinia mangostana* and  $\alpha$ -mangostin mediated silver nanoparticles, *Chemosphere* 272 (2021) 129794, <https://doi.org/10.1016/j.chemosphere.2021.129794>.
- [32] C.K. Githala, S. Raj, A. Dhaka, S.C. Mali, R. Trivedi, R. Phyto-fabrication of silver nanoparticles and their catalytic dye degradation and antifungal efficacy, *Front. Chem.* 10 (2022) 994721, <https://doi.org/10.3389/fchem.2022.994721>.
- [33] I. Fernando, Y. Zhou, Impact of pH on the stability, dissolution and aggregation kinetics of silver nanoparticles, *Chemosphere* 216 (2019) 297–305, <https://doi.org/10.1016/j.chemosphere.2018.10.122>.
- [34] Y. Wang, S. Wei, Green fabrication of bioactive silver nanoparticles using *Mentha pulegium* extract under alkaline: an enhanced anticancer activity, *ACS Omega* 7 (2021) 1494–1504, <https://doi.org/10.1021/acsomega.1c06267>.
- [35] A. Algarni, A. Fayomi, H. Al Garalleh, A. Afandi, K. Brindhadevi, A. Pugazhendhi, Nanofabrication synthesis and its role in antibacterial, anti-inflammatory, and anticoagulant activities of AgNPs synthesized by *Mangifera indica* bark extract, *Environ. Res.* 231 (2023) 115983, <https://doi.org/10.1016/j.envres.2023.115983>.
- [36] K. Sharma, S. Guleria, K.H. Salaria, A. Majeed, N. Sharma, K.D. Pawar, V.K. Thakur, V.K. Gupta, Photocatalytic and biological properties of silver nanoparticles synthesized using *Callistemon lanceolatus* leaf extract, *Ind. Crops Prod.* 202 (2023) 116951, <https://doi.org/10.1016/j.indcrop.2023.116951>.
- [37] Y. Shu, S. Li, C. Li, A. Liang, Z. Jiang, Liquid crystal@ nanosilver catalytic amplification—aptamer trimode biosensor for trace Pb<sup>2+</sup>, *Int. J. Mol. Sci.* 24 (2023) 2920, <https://doi.org/10.3390/ijms24032920>.
- [38] S. Link, M.A. El-Sayed, Size and temperature dependence of the plasmon absorption of colloidal gold nanoparticles, *J. Phys. Chem.* 103 (1999) 4212–4217, <https://doi.org/10.1021/jp984796o>.
- [39] N. Akaighe, S.W. Depner, S. Banerjee, V.K. Sharma, M. Sohn, The effects of monovalent and divalent cations on the stability of silver nanoparticles formed from direct reduction of silver ions by Suwannee River humic acid/natural organic matter, *Sci. Total Environ.* 441 (2012) 277–289, <https://doi.org/10.1016/j.scitotenv.2012.09.055>.
- [40] M. Danouche, H. El Arroussi, N. El Ghachtouli, Bioremoval of Acid Red 14 Dye by *Wickerhamomyces Anomalus* Biomass: Kinetic and Thermodynamic Study, Characterization of Physicochemical Interactions, and Statistical Optimization of the Biosorption Process, *Biomass Conv. Bioref.*, 2022, pp. 1–20, <https://doi.org/10.1007/s13399-022-02711-x>.
- [41] S.A. Khan, E.M. Bakhsh, A.M. Asiri, S.B. Khan, Synthesis of zero-valent Au nanoparticles on chitosan coated NiAl layered double hydroxide microspheres for the discoloration of dyes in aqueous medium, *Spectrochim. Acta Mol. Biomol. Spectrosc.* 250 (2021) 119370, <https://doi.org/10.1016/j.saa.2020.119370>.
- [42] J. Yang, S. Lu, H. Wu, H. Hu, Q. Miao, L. Huang, L. Chen, Y. Ni, Mussel-inspired magnetic dissolving pulp fibers toward the adsorption and degradation of organic dyes, *Front. Chem.* 10 (2022) 840133, <https://doi.org/10.3389/fchem.2022.840133>.
- [43] S. Chatterjee, X.Y. Lou, F. Liang, Y.W. Yang, Surface-functionalized gold and silver nanoparticles for colorimetric and fluorescent sensing of metal ions and biomolecules, *Coord. Chem. Rev.* 459 (2022) 214461, <https://doi.org/10.1016/j.ccr.2022.214461>.
- [44] N.D. Hai, N.M. Dat, D.B. Thinh, N.T. H Nam, N.T. Dat, M.T. Phong, N.H. Hieu, Phytosynthesis of silver nanoparticles using *Mangifera indica* leaves extract at room temperature: formation mechanism, catalytic reduction, colorimetric sensing, and antimicrobial activity, *Colloids Surf. B Biointerfaces* 220 (2022) 112974, <https://doi.org/10.1016/j.colsurfb.2022.112974>.
- [45] D. Abdelmoneim, G. Porter, W. Duncan, K. Lim, R. Easingwood, T. Woodfield, D. Coates, D. Three-dimensional evaluation of the cytotoxicity and antibacterial properties of alpha lipoic acid-capped silver nanoparticle constructs for oral applications, *Nanomaterials* 13 (2023) 705, <https://doi.org/10.3390/nano13040705>.
- [46] E. Matras, A. Gorczyca, S.W. Przemieniecki, M. Oćwieja, Surface properties-dependent antifungal activity of silver nanoparticles, *Sci. Rep.* 12 (2022) 18046, <https://doi.org/10.1038/s41598-022-22659-2>.